Identification of Novel Metabolites of Butadiene Monoepoxide in Rats and Mice

ARTICLE *in* CHEMICAL RESEARCH IN TOXICOLOGY · JANUARY 1999

Impact Factor: 3.53 · DOI: 10.1021/tx970175v · Source: PubMed

8 AUTHORS, INCLUDING:

Bernard Thomas Golding
Newcastle University
404 PUBLICATIONS **7,383** CITATIONS
SEE PROFILE

Peter J Boogaard
Shell Global
117 PUBLICATIONS **1,928** CITATIONS
SEE PROFILE

Identification of Novel Metabolites of Butadiene Monoepoxide in Rats and Mice

Kevan A. Richardson,† Melanie M. C. G. Peters,† René H. J. J. J. Megens,† Paul A. van Elburg,† Bernard T. Golding,‡ Peter J. Boogaard,† William P. Watson,*,† and Nico J. van Sittert*,†

Toxicology Department, Shell Research and Technology Centre, Shell International Chemicals, P.O. Box 38000, 1030 BN Amsterdam, The Netherlands, and Department of Chemistry, University of Newcastle upon Tyne, Newcastle upon Tyne NE1 7RU, U.K.

Received September 23, 1997

Differences in the metabolism of 1,3-butadiene (Bd) in rats and mice may account for the observed species difference in carcinogenicity. Previous studies of the metabolic fate of Bd have identified epoxide formation as a key metabolic transformation which gives 1,2-epoxy-3-butene (BMO), although some evidence of aldehyde metabolites is reported. In this study, male Sprague-Dawley rats and male B6C3F1 mice received single doses of [4-^{14}C]BMO at 1, 5, 20, and 50 mg/kg of body weight (0.014, 0.071, 0.286, and 0.714 mmol/kg of body weight). Analysis of urinary metabolites indicated that both species preferentially metabolize BMO by direct reaction with GSH when given by ip administration. The excretion of (*R*)-2-(*N*-acetyl-L-cystein-*S*-yl)-1-hydroxybut-3-ene (**IIa**), 1-(*N*-acetyl-L-cystein-*S*-yl)-2-(*S*)-hydroxybut-3-ene (**IIb**), 1-(*N*-acetyl-L-cystein-*S*-yl)-2-(*R*)-hydroxybut-3-ene (**IIc**), and (*S*)-2-(*N*-acetyl-L-cystein-*S*-yl)-1-hydroxybut-3-ene (**IId**) accounted for 48−64% of urinary radioactivity in rats and 46−54% in mice. The metabolites originating from the *R*-stereoisomer of BMO (**IIc and IId**) predominated over those arising from the *S*-stereoisomer (**IIa and IIb**) in both species. **IIc** was formed preferentially in mice and **IId** in rats. The corresponding mercaptoacetic acids, *S*-(1-hydroxybut-3-en-2-yl)mercaptoacetic acid (**IIf**) and *S*-(2-hydroxybut-3-en-1-yl)mercaptoacetic acid (**IIg**), were identified only in mouse urine (ca. 20% of the recovered radioactivity). 4-(*N*-Acetyl-L-cystein-*S*-yl)-1,2-dihydroxybutane (**Ia**), a metabolite derived from hydrolysis of BMO, accounted for 10−17% of the radioactivity in rat and 6−10% in mouse urine. 4-(*N*-Acetyl-L-cystein-*S*-yl)-2-hydroxybutanoic acid (**Ib**), 3-(*N*-acetyl-L-cystein-*S*-yl)propan-1-ol (**Ic**), and 3-(*N*-acetyl-L-cystein-*S*-yl)propanoic acid (**Id**), also derived from the hydrolysis of BMO, were only present in the rat. Metabolites of 1,2,3,4-diepoxybutane (DEB) were not detected after administration of BMO in rat or mouse urine. This study showed both quantitative and qualitative differences in the metabolism of BMO with varying doses and between species. The data aid in the safety evaluation of Bd and contribute to the interpretation of mathematical models developed for quantitative risk assessment and extrapolation of animals to humans.

Introduction

1,3-Butadiene (Bd)[1] is a carcinogen in rats and mice (*1*−*5*), with mice being much more sensitive than rats. In mice, tumors were noted at concentrations as low as 6 ppm Bd, while in rats, they occurred only after exposure to concentrations of >1000 ppm. In addition to the extreme susceptibility of mice compared to rats, the tumor pattern differed in both species. Part of the explanation for these observations may lie in differences in the metabolism of Bd and the DNA binding of reactive metabolites.

Studies of the metabolic fate of Bd in in vitro systems (*6*−*9*) and in animals (*10*−*17*) have identified epoxide formation as the key metabolic transformation which gives the monoepoxide, 1,2-epoxy-3-butene (BMO), and then, after further oxidation, the diepoxide, 1,2,3,4-diepoxybutane (DEB). These epoxides have the potential to alkylate biomolecules, including DNA, and thus are implicated in its carcinogenicity. DEB is seen as a highly significant metabolite since it is up to 100-fold more mutagenic than BMO in vitro (*18*) and has been shown to be responsible for DNA cross-links (*19*).

Studies using subcellular lung and liver fractions from humans, rats, and mice indicated that mouse microsomes metabolize Bd to BMO at a significantly faster rate than the microsomes from either rat or human tissues (*20, 21*). This is paralleled in vivo with mice that are able to

* To whom correspondence should be addressed.
† Shell International Chemicals.
‡ University of Newcastle upon Tyne.

[1] Abbreviations: Bd, 1,3-butadiene; BMO, 1,2-epoxy-3-butene; [^{14}C]-BMO, [4-^{14}C]-1,2-epoxy-3-butene; DEB, 1,2,3,4-diepoxybutane; EDB, 1,2-dihydroxy-3,4-epoxybutane; BSTFA, bis-silyl trifluoroacetamide; DMSO, dimethyl sulfoxide; HMPA, hexamethylphosphoramide; NAC, *N*-acetyl-L-cysteine; sa, specific radioactivity; TMSC, trimethylsilyl chloride; TMS, trimethylsilyl; triglyme, triethylene glycol dimethyl ether; **Ia**, 4-(*N*-acetyl-L-cystein-*S*-yl)-1,2-dihydroxybutane; **Ib**, 4-(*N*-acetyl-L-cystein-*S*-yl)-2-hydroxybutanoic acid; **Ic**, 3-(*N*-acetyl-L-cystein-*S*-yl)propan-1-ol; **Id**, 3-(*N*-acetyl-L-cystein-*S*-yl)propanoic acid; **IIa**, (*R*)-2-(*N*-acetyl-L-cystein-*S*-yl)-1-hydroxybut-3-ene; **IIb**, 1-(*N*-acetyl-L-cystein-*S*-yl)-2-(*S*)-hydroxybut-3-ene; **IIc**, 1-(*N*-acetyl-L-cystein-*S*-yl)-2-(*R*)-hydroxybut-3-ene; **IId**, (*S*)-2-(*N*-acetyl-L-cystein-*S*-yl)-1-hydroxybut-3-ene; **IIe**, 4-(*N*-acetyl-L-cystein-*S*-yl)-1-hydroxybut-2-ene; **IIf**, *S*-(1-hydroxybut-3-en-2-yl)mercaptoacetic acid; **IIg**, *S*-(2-hydroxybut-3-en-1-yl)mercaptoacetic acid.

10.1021/tx970175v CCC: $15.00
Published on Web 11/21/1998

achieve blood concentrations of BMO higher than those in rats when they are exposed to similar concentrations of Bd. The rates of oxidation of BMO to DEB by microsomes from mouse liver are also significantly greater than the rates obtained from rat or human microsomes (*20*, *21*).

Experiments in rats and mice have shown that BMO after ip administration undergoes reactions with GSH, following recognized biotransformation pathways, to produce the mercapturic acids: 1-(*N*-acetyl-L-cystein-*S*-yl)-2-hydroxybut-3-ene and 2-(*N*-acetyl-L-cystein-*S*-yl)-1-hydroxybut-3-ene (*22*). These mercapturic acids were also detected in the urine of rats, mice, and hamsters after inhalation exposure to 8000 ppm Bd for 2 h (*23*). A major metabolite identified in urine from either rats, mice, or monkeys and the only metabolite that could be detected in urine of Bd-exposed workers was 4-(*N*-acetyl-L-cystein-*S*-yl)-1,2-dihydroxybutane (*24*), which is thought to form by hydrolysis of BMO and subsequent addition of GSH. However, this metabolite was not identified after administration of BMO to rodents (*22*).

Nauhaus et al. (*25*) used NMR to analyze whole urine from rats and mice following inhalation exposure to ^{13}C-labeled Bd (800 ppm for 5 h) and reported the metabolites formed from hydrolysis and from direct reaction of BMO with GSH as well as those derived from DEB, in both species. In addition to these, 1-(*N*-acetyl-L-cystein-*S*-yl)-1-hydroxy-3-butene, 3-(*N*-acetyl-L-cystein-*S*-yl)propan-1-ol, and 3-(*N*-acetyl-L-cystein-*S*-yl)propanoic acid were found in mouse but not in rat urine with the suggestion that they may be formed via an additional metabolic pathway in the mouse involving aldehyde intermediates such as 3-butenal, crotonaldehyde, or acrolein rather than the epoxides BMO and DEB. Interestingly, PBPK models developed on the basis of the in vitro kinetics of biotransformation of Bd to BMO and BMO to DEB together with the rates of hydrolysis and GSH conjugation of these epoxides do not appear to predict experimentally determined levels of BMO and DEB in animals exposed to Bd (*26*). Better data fits were obtained when it was assumed that Bd metabolism proceeds through an additional pathway in which BMO does not play a central role.

A detailed understanding of metabolic fate is an essential component of the risk assessment of Bd. As part of our program of work on the characterization of Bd metabolic pathways, the nature of Bd metabolites bound to DNA, and the development of biomarkers for occupational exposure to Bd, we have examined the metabolism of [^{14}C]BMO in rats and mice. The principal objective of this work was to identify the urinary metabolites formed from BMO. Four dose levels were examined, from 1 to 50 mg/kg, including those previously reported (*22*). These dose levels were higher than the equivalent levels of BMO measured in blood produced by rats and mice during 2−6 h exposures to Bd atmospheres (21). However, they afforded metabolites in sufficient quantities to determine the nature of these components.

Methods

Safety. BMO (1,2-epoxy-3-butene, CAS registry number 930-22-3) is a primary metabolite of Bd (*10*). BMO is mutagenic in vitro (*27*, *28*) and a suspected carcinogen. Because of the volatility of the compound, all work must be performed in a well-ventilated fume hood. Protective clothing, including gloves, should be worn to prevent skin absorption.

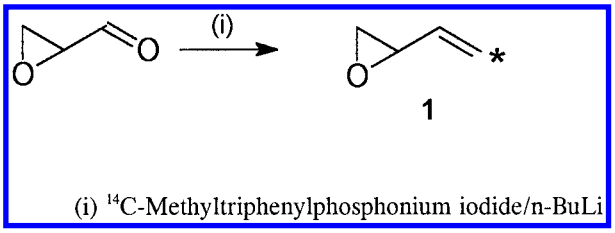

Figure 1. Synthesis of ^{14}C-labeled BMO (the asterisk denotes the position of the radiolabel).

Chemicals. Unless otherwise stated, chemicals were of the highest available purity. Solvents used for HPLC were HPLC grade. All solvents used for other purposes were analytical (PA) grade. Triethylene glycol dimethyl ether (triglyme, Aldrich) was distilled from sodium hydride. Methyltriphenylphosphonium iodide (Aldrich) was dried in vacuo over phosphorus pentoxide. 3-(*N*-Acetyl-L-cystein-*S*-yl)propan-1-ol (**Ic**) was a gift from J. P. Kehrer (College of Pharmacy, University of Texas at Austin, Austin, TX) (*29*).

Radiochemical. [4-^{14}C]BMO (**1**) was synthesized from [^{14}C]-methyltriphenylphosphonium iodide and racemic glycidaldehyde (*30*) using the Wittig reaction (Figure 1). A slurry of methyltriphenylphosphonium iodide (101.7 mg, 0.25 mmol) and [^{14}C]-methyltriphenylphosphonium iodide [Amersham International, 88.3 mg, 0.22 mmol, specific radioactivity (sa) of 58 mCi/mmol] in dry triglyme was prepared in a reaction flask under a dry nitrogen atmosphere. The mixture was cooled to −40 °C, and *n*-butyllithium (Aldrich, titrated as a 2.0 M solution in pentane, 258 μL, 0.52 mmol) was added dropwise by syringe. After the mixture was stirred at −40 °C for 30 min and at 0 °C for 30 min, volatiles were removed under reduced pressure (7×10^{-3} mmHg) at 0 °C over the course of 3 h. The residue was dissolved in hexamethylphosphoramide (HMPA, Aldrich, 480 μL, 2.76 mmol). The HMPA solution was then stored overnight at −22 °C under a dry nitrogen atmosphere. The stored mixture was recooled to −40 °C, and a solution of glycidaldehyde (30.8 μL, 0.43 mmol) in dry triglyme (1.5 mL) was added dropwise by syringe. After the mixture was stirred at −40 °C for 30 min and then at 0 °C for 30 min, [^{14}C]BMO was distilled from the reaction mixture under reduced pressure (0.02 mmHg) and trapped in a receiving vessel cooled to −196 °C. Triglyme was trapped in two preceding vessels cooled to −45 °C. The distillation was controlled such that the temperature of the reaction flask was maintained at −30 °C for 60 min, −10 °C for 30 min, and then at 0 °C for 60 min. The contents of the receiving vessel were redistilled under reduced pressure and at room temperature into a small volume of dimethyl sulfoxide (DMSO, 200 μL) previously cooled to −196 °C. The resulting solution was allowed to warm to room temperature and reach atmospheric pressure using ingress of nitrogen. The reaction yielded 4.90 mg (16% based on glycidaldehyde) of [4-^{14}C]BMO with a radiochemical purity of >99% as indicated by GC and HPLC analysis. GC was performed on a Poraplot Q (Chrompack, 25 m × 0.32 mm, 1.0 μm film thickness) column. The initial oven temperature was 115 °C. After 10 min, the temperature was increased at a rate of 70 °C/min to 200 °C. Radioactivity was detected using a RAGA 90 (Raytek Scientific Ltd.) detector in the reducing mode. The chemical identity was confirmed by comparison of the retention time of the radioactive material with that of unlabeled BMO (12 min) and MS [EI *m*/*z* 70 ($M^{+\bullet}$) and 69 (M − 1)]. HPLC was performed on a reversed phase analytical column (Supelcosil LC-18, 250 mm × 4.6 mm, 5 μm) eluted with acetonitrile (25%) in water for 10 min, which was increased to 100% acetonitrile over the course of 10 min, at a flow rate of 1 mL/min (retention time of 11 min). Radioactivity was monitored by a flow-through detector (Ramona 90, Raytek Scientific Ltd.). GC analysis showed that BMO was prepared with a chemical purity of 75% with benzene as the major impurity. The chemical purity of the BMO used for dosing was

>94% after the sa of the [^{14}C]BMO was adjusted by addition of unlabeled BMO (see dose solution below).

Synthesis of Reference Metabolites. (1) 4-(*N*-Acetyl-L-cysteinyl-*S*-yl)-1,2-dihydroxybutane (Ia). This chemical was synthesized according to the procedures described by Sabourin et al. (*23*) from 4-(*N*-acetyl-L-cysteinyl-*S*-yl)-1-acetoxybutan-2-one. 4-(*N*-Acetyl-L-cysteinyl-*S*-yl)-1-acetoxybutan-2-one was prepared from *N*-acetyl-L-cysteine sodium salt and acetoxymethyl vinyl ketone, which was obtained as described by Hennion and Kupiecki (*31*). 4-(*N*-Acetyl-L-cysteinyl-*S*-yl)-1,2-dihydroxybutane (**Ia**) was isolated by preparative reversed phase HPLC (Hichrom, Zorbax ODS column, 250 mm × 20 mm, 10 μm) eluting with water containing acetonitrile (7.5%) and trifluoroacetic acid (0.1%) at a flow rate of 10 mL/min (retention time of 10 min) which yielded 118 mg (64%) of **Ia** with a purity of >95%. Trimethylsilyl (TMS) derivative of **Ia** (see below for derivatization method): EI *m*/*z* 452 (M − 15), 377, 362, 308, 228, 202, 129, 73 (base peak), 43; CI (methane) *m*/*z* 468 (M + H); ^{1}H NMR **of Ia** (200 MHz, CD_3OD) δ 4.58−4.52 (1H, m, αC-cys), 3.78−3.62 (1H, m, CHOH), 3.58 (1H, dAB, J_{AB} = 11.7 Hz, J_{vic} = 3.7 Hz, H_A of CH_AH_BOH), 3.48 (1H, dAB, J_{AB} = 11.7 Hz, J_{vic} = 6.7 Hz, H_B of CH_AH_BOH), 3.10 (1H, dAB, J_{AB} = 14.0 Hz, J_{vic} = 6.0 Hz, H_A of βC-cys), 2.95 (1H, ddAB, J_{AB} = 14.0 Hz, J_{vic} = 7.4 Hz and ^3J = 1.4 Hz, H_B of βC-cys), 2.8−2.6 (2H, m, SCH_2CH_2), 2.06 (3H, s, $COCH_3$), 1.8−1.6 (2H, m, SCH_2CH_2); ^{1}H NMR of 4-(*N*-acetyl-L-cysteinyl-*S*-yl)-1-acetoxybutan-2-one (200 MHz, CD_3OD) δ 4.86 (2H, s, CH_2OCO), 4.58−4.42 (1H, m, αC-cys), 3.07 (1H, d_{AB}, J_{AB} = 14.9 Hz, J_{vic} 6.9 Hz, H_A of βCH_AH_B-cys), 2.92 (1H, d_{AB}, J_{AB} = 14.9 Hz, J_{vic} = 4.9 Hz, $H_B\beta$C-cys), 2.9−2.75 (4H, m, CH_2CH_2), 2.15 (3H, s, $OCOCH_3$), 2.02 (3H, s, $NCOCH_3$).

(2) *N*-Acetyl-L-cysteine S-Conjugates of BMO (IIa−IIe). A mixture of regio- and stereochemical isomers of the *N*-acetyl-L-cysteine S-conjugates of BMO was prepared from NAC and BMO in acetone/water (1:1) at pH 8.5 as described by Elfarra et al. (*22*). Four major products were isolated by HPLC and derivatized using BSTFA (bis-silyl trifluoroacetamide)/10% TMSC (trimethylsilyl chloride). GC/MS analysis of derivatized 2-(*N*-acetyl-L-cystein-*S*-yl)-1-hydroxybut-3-ene (C-2 isomers, **IIa** and **IId**) afforded the following ions: CI (methane) *m*/*z* 378 (M + H); EI *m*/*z* 362 (M − 15), 318, 308, 287, 234, 228, 103 (CH_2=O^+SiMe_3), 73 (base peak), where the ion at *m*/*z* 103 was characteristic of the derivatized primary alcohol. Derivatized 1-(*N*-acetyl-L-cystein-*S*-yl)-2-hydroxybut-3-ene (C-1 isomers, **IIb** and **IIc**) afforded the following ions: CI (methane) *m*/*z* 378 (M + H); EI *m*/*z* 362 (M − 15), 321, 308, 142, 129 (base peak, CH_2=CHCH=O^+SiMe_3), where the ion at *m*/*z* 129 was characteristic of the derivatized secondary allylic alcohol. The relative elution of the major components under the HPLC conditions described below (HPLC of urine metabolites) was **IIa** (C-2 isomer), **IIb** (C-1 isomer), **IIc** (C-1 isomer), and **IId** (C-2 isomer). A minor component also present in the mixture and which afforded the same molecular ion (M + H) as the C-1 and C-2 isomers after TMS derivatization was identified as 4-(*N*-acetyl-L-cystein-*S*-yl)-1-hydroxybut-2-ene (**IIe**) on the basis of the work of Elfarra et al. (*22*): CI *m*/*z* 378 (M + H); EI *m*/*z* 362 (M − 15), 308, 234, 142, 202, 176,159, 143, 73.

(3) (*S*)-1-(Tosyloxy)-2-hydroxybut-3-ene. Tosyl chloride (recrystallized from benzene, 2.2 g, 11.6 mmol) was added to a solution of (*S*)-1,2-dihydroxybut-3-ene (0.976 g, 11.4 mmol, Across Organics) in anhydrous pyridine (20 mL) at 0 °C. The resulting mixture was stirred for 6 h at 0 °C under nitrogen and stored at 4 °C overnight. Chloroform (35 mL) and water (15 mL) were added, and the mixture was acidified to pH 3−4 by addition of HCl (0.5 M). The organic layer was washed with water (2 × 15 mL), dried with $MgSO_4$, filtered, and evaporated to dryness at reduced pressure. The residue was purified by column chromatography (silica gel) using a mixture of hexane and ethyl acetate (2:1) as the eluant. The resulting white solid had a purity of 92% by ^{1}H NMR and contained 8% of the ditosylate: ^{1}H NMR (200 MHz, $CDCl_3$) δ 7.8 (2H, d, J = 10.0 Hz, ArH), 7.4 (2H, d, J = 10.0 Hz, ArH), 5.9−5.7 (1H, m, CH=), 5.45−5.2 (2H, m, =CH_2), 4.46−4.38 (1H, m, CHOH), 4.1 (1H, d_{AB}, J_{AB} = 12.5 Hz, J_{vic} = 3.8 Hz, H_A of $CH_AH_B\overline{O}$), 3.9 (1H, d_{AB}, J_{AB} = 12.5 Hz, J_{vic} = 9.7 Hz, H_B of CH_AH_BO), 2.5 (3H, s, CH_3); ^{13}C NMR (250 MHz, CD_3OD/D_2O) δ 144.8 (s, Ar), 134.7 (d, CH=), 131.7 (s, Ar), 129.0 (d, Ar), 126.9 (d, Ar), 115.8 (t, =CH_2), 72.1 (t, CH_2O), 68.9 (d, CHOH), 19.5 (q, CH_3).

(4) 2-(*R*)-(*N*-Acetyl-L-cystein-*S*-yl)-1-hydroxybut-3-ene (IIa) and 1-(*N*-Acetyl-L-cystein-*S*-yl)-2-(*S*)-hydroxybut-3-ene (IIb). (*S*)-1-(Tosyloxy)-2-hydroxybut-3-ene (0.258 g, 1 mmol) was dissolved in a mixture of CD_3OD (2.5 mL) and D_2O (0.9 mL) in an NMR tube. A solution of NAC (0.161 g, 1 mmol) and NaOH (0.08 g, 2 mmol) in D_2O (0.5 mL) was then added. ^{1}H NMR indicated that the tosylate was initially converted to the corresponding (*S*)-epoxide after the addition of base: ^{1}H NMR (CD_3OD/D_2O) δ 5.55−5.50 (2H, m, =CH_2), 5.32−5.25 (1H, m, =CH), 3.35−3.30 (1H, m, CHO), 2.95−2.92 (1H, m, CH_2O), 2.65−2.61 (1H, m, CH_2O) (*32*). After the mixture was heated at 70 °C for 4 h, all signals corresponding to the presence of the intermediate (*S*)-epoxide disappeared. LC/MS of the reaction mixture indicated two components. The first eluting component afforded ions at *m*/*z* 234 (M + H), 216, 192, 174, 162, 130, 122, and 105. This component cochromatographed with the first eluting component from the chemical reaction of NAC with racemic BMO (see above), identifying it as a C-2 diastereoisomer, 2-(*N*-acetyl-L-cystein-*S*-yl)-1-hydroxybut-3-ene (**IIa**), and which afforded the same ions under the electrospray MS conditions used. The second component afforded ions at *m*/*z* 234 (M + H), 216, 174, 162, and 130. This component cochromatographed with the second eluting component from the chemical reaction of NAC with racemic BMO (see above), identifying it as a C-1 diastereoisomer, 1-(*N*-acetyl-L-cystein-*S*-yl)-2-hydroxybut-3-ene (**IIb**), and which afforded the same ions under the electrospray MS conditions used. The ion fragment patterns for the C-1 and C-2 diastereoisomers showed minor differences, supporting the cochromatography experiments. The C-2:C-1 ratio was measured as ca. 2:1. As the reaction of GSH at C-1 retains the configuration of the (*S*)-epoxide in forming the (*S*)-alcohol, the stereochemical assignment of **IIb** was 1-(*N*-acetyl-L-cystein-*S*-yl)-2-(*S*)-hydroxybut-3-ene. Reaction at C-2 is expected to occur with inversion at this center, which identified **IIa** as (*R*)-2-(*N*-acetyl-L-cystein-*S*-yl)-1-hydroxybut-3-ene: ^{13}C NMR of the mixture **IIa** (250 MHz, CD_3OD/D_2O) δ 177.7 (s, CO), 173.9 (s, CO), 140.8 or 137.5 (d, =CH), 118.6 or 116.6 (t, =CH_2), 64.9 (t, CH_2O), 56.2 (d, αC-cys), 52.3 (d, SCH), 36.5 or 34.0 (t, βC-cys), 23.5 (q, CH_3); ^{13}C NMR of the mixture **IIb** (250 MHz, CD_3OD/D_2O) δ 177.7 (s, CO), 173.9 (s, CO), 140.8 or 137.5 (d, =CH), 118.6 or 116.6 (t, =CH_2), 73.4 (d, CHOH), 56.2 (d, αC-cys), 40.3 (t, SCH), 36.5 or 34.0 (t, βC-cys), 23.5 (q, CH_3).

(5) 1,2-Dihydroxy-3,4-epoxybutane. A solution of 1,2-dihydroxybut-3-ene (100 mg, 1.14 mmol) in dichloromethane (1 mL) was added to *m*-chloroperbenzoic acid (100%, 234 mg, 1.36 mmol) in dichloromethane (1 mL) under nitrogen at 0 °C. The reaction mixture was stirred overnight and allowed to warm slowly from 0 °C to room temperature. After the mixture was cooled with ice/water and filtration, dichloromethane was removed at 30 °C under reduced pressure. The residue was reconstituted in D_2O (1 mL), filtered, and adjusted to pH 7 and the mixture of stereoisomers analyzed by ^{1}H NMR (200 MHz, D_2O): δ 3.7−3.5 (2H, m, $HOC\underline{H}_2$), 3.5−3.4 (1H, m, $C\underline{H}OH$), 3.1−3.05 (1H, m, OCH), 2.9−2.7 (2H, m, OCH_2); ^{13}C NMR (300 MHz, D_2O) δ 72.2 and 70.5 (d, CHO), 63.0 (t, CH_2OH), 53.7 and 52.7 (d, CHOH), 45.3 and 45.0 (t, CH_2OH).

(6) 4-(*N*-Acetyl-L-cystein-*S*-yl)-1,2,3-trihydroxybutane. A solution of NAC (230 mg, 1.41 mmol) in deionized water (0.5 mL) was added to NaOH (91 mg, 2.28 mmol) dissolved in deionized water (1.0 mL). After the mixture was stirred for 5 min at room temperature, a freshly made solution of 1,2-dihydroxy-3,4-epoxybutane (146 mg, 1.41 mmol) in deionized water (2.5 mL) was added. The pH of the solution was measured as >10. The reaction mixture was stirred for 4 h at room temperature, and then the solvent was removed under

reduced pressure by rotary evaporation to give a semisolid colorless residue. LC/MS (conditions below) gave a broad peak (retention time of 5−7 min) with ions at *m*/*z* 268 (M + H), 250, 232, 192, 162, 130, and 121. This was consistent with the expected products 4-(*N*-acetyl-L-cystein-*S*-yl)-1,2,3-trihydroxybutane and 3-(*N*-acetyl-L-cystein-*S*-yl)-1,2,4-trihydroxybutane. The product was isolated by SAX HPLC (Whatman, Partisil, SAX column, 250 mm × 10 mm, 10 μm) using ammonium formate buffer (1 mM) at pH 3 (prepared by addition of 1 L of 3.8 mL/L formic acid to 10 mL of 0.1 M ammonium formate) containing formic acid (0.5 M, 5%) at a flow rate of 2.5 mL/min as the eluant (retention time of 15 min). The HPLC solvent was removed by rotary evaporation under reduced pressure at 40 °C to give a colorless oil. ^{13}C NMR identified this isolated material as a mixture of the diastereoisomers of 4-(*N*-acetyl-L-cystein-*S*-yl)-1,2,3-trihydroxybutane. No signals from the other isomer, 3-(*N*-acetyl-L-cystein-*S*-yl)-1,2,4-trihydroxybutane were present: ^{1}H NMR of the isolated component (250 MHz, D_2O) δ 4.6−4.5 (1H, m, αC-cys), 3.8−3.5 (4H, m, OCH_2, OCH), 3.26−2.60 (4H, m, SCH_2), 2.02 (3H, s, $COCH_3$); ^{13}C NMR of the isolated component (300 MHz, D_2O) δ 174.4 and 174.3 (s, COOH), 166.3 (s, NHCO), 73.7, 73.05, 73.0, 71.0, 70.8, 70.4 and 70.3 (d, CHOH), 62.9 and 62.7 (t, CH_2O), 53.03 and 53.0 (d, αC-cys), 35.6, 35.55, 35.3, 33.6, 33.4, 33.33, 33.27 (t, SCH_2), 21.8 (q, CH_3).

Dosing Solution. [4-^{14}C]BMO was diluted with unlabeled BMO (Aldrich) in DMSO as the dose vehicle. The sa was determined by GC measurement of the chemical concentration by comparison with a BMO standard curve and measurement of the radiochemical concentration by liquid scintillation counting. Several batches of [^{14}C]BMO were prepared in this manner each with a target sa of 1 mCi/mmol. BMO was shown to be stable with no losses when it was stored in the DMSO formulation at −5 or −20 °C for up to 21 days. Target dose levels were 1, 5, 20, or 50 mg/kg [^{14}C]BMO which are equivalent to 0.014, 0.071, 0.286, and 0.714 mmol/kg, respectively. Actual received values were based on the assay of the dose solutions before and after the completion of dosing. Rats received 1, 5, 18, or 51 mg/kg [^{14}C]BMO with a sa of 1.3, 1.1, 0.8, and 1.0 mCi/mmol, respectively. Mice received 1, 5, 21, or 54 mg/kg [^{14}C]BMO with a sa of 1.3, 1.1, 0.8, and 1.0 mCi/mmol, respectively.

Animal Dosing and Sample Collection. Male B6C3F1 mice (20−30 g) and male Sprague-Dawley rats (200−300 g) obtained from Charles River (Manston, Kent, U.K.) were given a single dose of [4-^{14}C]BMO in DMSO (1.5−2 mL/kg) by ip injection. The 1, 5, and 50 mg/kg [^{14}C]BMO dose groups consisted of three rats or five mice per dose level. The 20 mg/kg [^{14}C]BMO group consisted of six rats or 25 mice. A single control rat and five mice were maintained for the duration of the experiment and were used to provide background values for the determination of tissue residues in treated animals. After dosing, rats were maintained individually and mice in groups of five in metabolism cages in fume hoods. Animals had free access to food (LAD2) and water. Feces and urine were collected separately at 4 °C and sampled 6, 24, and 48 h after dosing. Cages were rinsed with methanol/water (2 × 25 mL, 1:1 v/v) 48 h after dosing. Blood and tissues (lung, liver, heart, fat, testes, kidneys, adrenal glands, spleen, muscle, femoral bone marrow, brain, and gastrointestinal tract) were removed at the end of the 48 h holding period to determine the distribution of radioactivity between the tissues. Samples were stored at −80 °C until further analysis.

Quantitation of Radioactivity. Liquid samples (2 × 10−200 μL) were taken up in Optiphase "Safe" (LKB, 20 mL) or Ultima Gold scintillation fluid (Canberra-Packard) and measured using a Canberra-Packard (model 2200CA) liquid scintillation counter. Radioactivity in blood, tissue, and feces was determined by oxygen combustion using a Canberra-Packard 306M combustor. Duplicate or triplicate tissue samples of ca. 100−200 mg were analyzed except for whole blood, bone marrow, adrenal glands, and fat where ca. 25−50 mg samples were used. The combustion efficiency was determined using commercial standards (Amersham) or control tissues spiked with a ^{14}C standard (Canberra-Packard).

HPLC of Urine Metabolites. BMO metabolites in whole urine or in isolated fractions were analyzed by reversed phase HPLC using a YMC ODS AQ column (250 mm × 4.6 mm, 5 μm) and elution with 1 mM ammonium formate buffer at pH 3 (prepared by addition of 1 L of 3.8 mL/L formic acid to 10 mL of 0.1 M ammonium formate) containing acetonitrile (9%) at a flow rate of 1 mL/min. Radioactivity was detected using a flow-through radiodetector (Ramona 90, solid cell).

Enzymatic Treatment of Urine. Aliquots of urine (rat, 0.5 mL; mouse, 0.2 mL) were diluted with an equal volume of ammonium acetate buffer (0.2 M, pH 5.0) and incubated with an equal volume of glucurase (5000 units/mL β-glucuronidase, ex. bovine liver, Sigma), sulfatase (0.64 mg, type H-1, ex *Helix pomatia*, 18 000 units/g, Sigma), or acylase I (6 mg, 7000 units/mg, Sigma) overnight at 37 °C. The reaction was stopped by cooling to −20 °C. Metabolic profiles were analyzed by radio-HPLC and compared to those of control samples incubated without enzyme. The activity of the sulfatase and glucuronidase enzymes was checked by the addition of *p*-nitrophenyl sulfate or phenolphthalein glucuronic acid (Sigma) after overnight incubation. After a further 30 min, sodium hydroxide (1.0 M, 0.5 mL) was added, and the development of a yellow (*p*-nitrophenol) or pink (phenolphthalein) color indicated the viability of the enzymes.

Isolation of Urinary Components. Combined urine samples were freeze-dried, reconstituted in half of the original volume of acetonitrile/water (1:4 v/v), and centrifuged. The supernatant was removed and the precipitate washed twice with water. The assay of the supernatant and the washes indicated that 95% of the original radioactivity was recovered in the supernatant. Washed urine samples were fractionated by reversed phase preparative HPLC with 1 mM ammonium formate buffer (pH 3) containing acetonitrile (9%) at a flow rate of 2.5 mL/min using a Hichrom ODS (250 mm × 10 mm, 10 μm) column for rat urine and at a flow rate of 10 mL/min using a YMC ODS AQ (250 mm × 20 mm, 5 μm) column for mouse urine. Fractions were freeze-dried and reconstituted in methanol or methanol/water.

Chemical Derivatization of Reference Chemicals and Metabolites. Samples of reference chemicals or isolated metabolite fractions were evaporated to dryness at 30−40 °C under nitrogen, redissolved in dry acetonitrile (50 μL), and evaporated to dryness, again. For trimethylsilylation, the silylating reagent (BSTFA/10% TMCS, 100 μL, Pierce) was added and the sample heated at 60 °C for 15 min, followed by immediate analysis. Alternatively, dry samples of isolated metabolite fractions were methylated by the addition of methanol/HCl (1 mL of acetyl chloride added to 10 mL of methanol) and heating to 60 °C for 1 h. Samples were cooled, evaporated to dryness at 40−50 °C under nitrogen, and dissolved in ethyl acetate for analysis. A fraction of the methylated product was acetylated by adding acetic anhydride/triethylamine/acetone (1:2:5 v/v/v) and heating at 60 °C for 15 min. After cooling and removal of solvents at 40−50 °C under nitrogen, the derivatized metabolites were dissolved in ethyl acetate and analyzed by GC/MS.

GC/MS of Reference Chemicals and Urine Metabolites. For GC analysis (Hewlett-Packard 5890 series II) of derivatized samples, we used an HP-5 column (Hewlett-Packard, 25 m × 0.32 mm, 1.05 μm film thickness), on-column injection, and helium as a carrier gas at a flow rate of 1 mL/min. The initial oven temperature was 80 °C. After 1 min, the temperature was increased at a rate of 40 °C/min to 250 °C. The flow was split 10:1 to on-line MS (Hewlett-Packard MSD 5971A). The radioactivity in the remainder of the flow was mixed with helium (2.5 mL/min) and hydrogen gas (4 mL/min) and measured using a RAGA 90 detector in the reducing mode with methane (35 mL/min) as a counting gas. The combination of radioactivity detection with MS analysis ensured the correct selection of metabolites in samples which contained multiple components.

Table 1. Elimination of Radioactivity in Urine and Feces of Male Sprague-Dawley Rats and Male B6C3F1 Mice after a Single ip Administration of 1, 5, 20, or 50 mg/kg [4-^{14}C]BMO[a]

	urine 0−6 h	feces 0−6 h	urine 0−48 h	feces 0−48 h	cage wash 48 h	total 48 h
rat dose level (mg/kg) (mmol/kg)						
1 (0.014)	40 ± 8	2 ± 0.5	47 ± 9	5 ± 2	1 ± 0.5	53 ± 11
5 (0.071)	41 ± 2	2 ± 0.4	48 ± 3	5 ± 2	1 ± 0.4	53 ± 5
20 (0.286)	45 ± 3	1 ± 0.2	52 ± 4	5 ± 1	1 ± 0.2	58 ± 4
50 (0.714)	41 ± 3	1 ± 0.2	51 ± 4	5 ± 2	1 ± 0.2	57 ± 6
			50 ± 2[b]	5	1	55 ± 2
mouse dose level (mg/kg) (mmol/kg)						
1 (0.014)	35	1	53	2	1	57
5 (0.071)	41	2	48	2	2	55
20 (0.286)	54 ± 5	2 ± 0.5	62 ± 4	2 ± 0.4	1 ± 0.7	67 ± 4
50 (0.714)	16	1	39	4	4	47
			52 ± 8[b]	3 ± 1	2 ± 1	57 ± 7

[a] Values are expressed as the mean percentage of dose excreted with the standard deviation (SD) at each time point (n = 3 or 6 rats, n = 5 mice). [b] Mean and SD using the four dose groups.

For further identification, derivatized samples were analyzed using a gas chromatograph coupled to a Hewlett-Packard Engine mass spectrometer (HP5989A). A DB-5 column (30 or 60 m × 0.25 mm, 0.25 μm film thickness) was used with split and/or splitless (240 °C) injection. The initial oven temperature was 40 °C. After 1 min, the temperature was increased at a rate of 20 °C/min to 220 °C.

LC/MS of Reference Chemicals and Urine Metabolite Standards. Reference chemicals or [^{14}C]BMO metabolites in whole urine and isolated fractions were separated by reversed phase HPLC using a YMC ODS AQ column (250 mm × 4.6 mm, 5 μm) by eluting with 1 mM ammonium formate buffer (pH 3) containing acetonitrile (9%) at a flow rate of 1 mL/min. The flow was split to 150 μL/min for mass spectrometry (VG Quattro triple-quadrupole instrument, electrospray ionization, using a source temperature of 100 °C and a cone voltage of 20 eV). The remainder of the flow was monitored by a flow-through radiodetector (Ramona 90).

Results

Animal Observations. Mild signs of toxicity, salivation and hunched and unkempt appearance, were observed in rats soon after receiving doses of [^{14}C]BMO of ≥20 mg/kg. These effects disappeared approximately 60−90 min after dosing. In contrast, mice showed no signs of toxicity after administration of equivalent doses of BMO. All animals appeared healthy and were eating and drinking normally during the 48 h holding period in metabolism cages.

Excretion of Radioactivity. A summary of the excretion of ^{14}C radioactivity following a single administration of [^{14}C]BMO to rats and mice is given in Table 1. The urinary elimination of radioactivity was rapid with the greatest proportion excreted in the first 6 h at all doses examined. In the rat, 41−45% of the radioactivity was excreted 0−6 h after dosing, with a further 4−10% of the dose being excreted between 6 and 24 h and 1−2% between 24 and 48 h. In the mouse, 35−54% of the radioactivity was excreted 0−6 h after dosing. An exception was the highest dose group of mice where only 16% of the administered dose was recovered in the 0−6 h urine due to loss of urine in the food hopper. After some modification, entry to the food hopper was restricted and remaining sampling intervals contained levels of radioactivity similar to those in the other dose groups (5−16% of the dose excreted between 6 and 24 h and 1−5% between 24 and 48 h). Recoveries in cage washes 48 h after dosing accounted for 1−4% of the administered radioactivity and were included in the urinary recoveries. A minor fraction (2−5%) of the administered radioactivity was recovered in the feces of both rats and mice. The metabolism cages were open systems; thus, exhaled [^{14}C]-BMO, [^{14}C]CO_2, or other ^{14}C volatiles were not collected. These volatile products, together with the small proportion of radioactivity associated with the tissues [ca. 8% of the administered radioactivity for rats using the highest dose group as an example (Table 2) and ca. 0.5% of the administered radioactivity for mice using the highest dose group as an example (Table 3)], probably accounted for the remainder of the administered radioactivity.

Table 2. Tissue and Blood Levels of Radioactivity Expressed as Nanomoles of [^{14}C]BMO Equivalents per Gram of Tissue with the Standard Deviation (n = 3 or 6) after a Single ip Administration of 1, 5, 20, or 50 mg/kg [4-^{14}C]BMO to Male Sprague-Dawley Rats

	average BMO equivalents (nmol) per gram of tissue			
rat tissue	1 mg/kg (0.014 mol/kg)	5 mg/kg (0.071 mol/kg)	20 mg/kg (0.286 mol/kg)	50 mg/kg (0.714 mol/kg)
adrenal	4.2 ± 1.1	17 ± 2.0	91 ± 51	167 ± 29 (0.003)[a]
fat	3.8 ± 2.3	15 ± 0.2	63 ± 16	160 ± 29 (1.25)[b]
bone marrow	2.2 ± 0.5	8.2 ± 0.9	32 ± 6.2	95 ± 14
brain	0.9 ± 0.2	3.5 ± 0.4	21 ± 5.2	59 ± 7.7 (0.05)[a]
heart	1.4 ± 0.15	8.3 ± 0.4	28 ± 4.8	83 ± 4.2 (0.05)[a]
kidney	1.8 ± 0.2	8.9 ± 0.8	35 ± 4.5	88 ± 11 (0.12)[a]
liver	8.6 ± 0.9	35 ± 14	171 ± 47	386 ± 2.4 (3.46)[a]
lung	1.7 ± 0.3	9.4 ± 1.5	33 ± 6.0	95 ± 18 (0.08)[a]
muscle	1.0 ± 0.2	4.2 ± 0.3	15 ± 4.0	45 ± 8.7
spleen	1.8 ± 0.2	8.2 ± 0.8	32 ± 4.2	101 ± 16 (0.04)[a]
testes	1.0 ± 0.1	4.1 ± 0.7	16 ± 4.2	50 ± 4.2 (0.08)[a]
blood	1.8 ± 0.3	28 ± 10	67 ± 28	161 ± 29 (2.5)[c]

[a] These results are expressed as a proportion (%) of the administered radioactivity and whole tissue weight. [b] This result is expressed as a proportion (%) of the administered radioactivity and assuming that fat accounts for approximately 5% of the body weight (250 g rats). [c] This result is expressed as a proportion (%) of the administered radioactivity and assuming that blood accounts for approximately 10% of the body weight (250 g rats).

Distribution of Radioactivity in Tissues and Blood. The data for the radioactivity remaining in blood and tissues 48 h after dosing of rats and mice are shown in Tables 2 and 3, respectively. Residue levels (picomoles of [^{14}C]BMO equivalents per gram of tissue) increased in all tissues with increasing doses for both rats and mice. Generally, rats had higher (up to ca. 10 times) levels of

Table 3. Tissue and Blood Levels of Radioactivity Expressed as Nanomoles of [^{14}C]BMO Equivalents per Gram of Tissue with the Standard Deviation (n = 3 or 5) after a Single ip Administration of 1, 5, 20, or 50 mg/kg [4-^{14}C]BMO to Male B6C3F1 Mice

	average BMO equivalents (nmol) per gram of tissue			
mouse tissue	1 mg/kg (0.014 mol/kg)	5 mg/kg (0.071 mol/kg)	20 mg/kg (0.286 mol/kg)	50 mg/kg (0.714 mol/kg)
adrenal	3.7	21	48 ± 5.0	90 (0.001)[a]
fat	0.7 ± 0.1	4.2 ± 0.1	14 ± 6.6	22 ± 2.7 (0.04)[b]
bone marrow	3.9	8.2	32 ± 7.4	61
brain	0.6 ± 0.05	1.9 ± 0.1	7.2 ± 0.2	20 ± 0.5 (0.02)[a]
heart	0.6 ± 0.02	2.9 ± 0.3	9.5 ± 0.7	24 ± 0.8 (0.02)[a]
kidney	1.0 ± 0.1	4.0 ± 0.1	11 ± 1.2	32 ± 2.8 (0.06)[a]
liver	1.1 ± 0.2	5.1 ± 0.5	13 ± 0.5	35 ± 2.4 (0.27)[a]
lung	0.8 ± 0.05	3.2 ± 0.1	12 ± 1.1	23 ± 2.3 (0.03)[a]
muscle	0.4 ± 0.03	2.0 ± 0.2	5.7 ± 0.9	16 ± 1.8
spleen	1.0 ± 0.1	3.5 ± 0.6	12 ± 2.0	29 ± 4.8 (0.01)[a]
testes	0.6 ± 0.01	1.9 ± 0.2	7.6 ± 0.7	17 ± 0.6 (0.01)[a]
blood	0.6	2.0	7.3 ± 1.1	21 (0.07)[c]

[a] These results are expressed as a proportion (%) of the administered radioactivity and whole tissue weight. [b] This result is expressed as a proportion (%) of the administered radioactivity and assuming that fat accounts for approximately 5% of the body weight (25 g mice). [c] This result is expressed as a proportion (%) of the administered radioactivity and assuming that blood accounts for approximately 10% of the body weight (25 g mice).

tissue residues than mice at equivalent dose levels with the exception of bone marrow and adrenal glands. In rats, the highest levels of tissue residues were seen in the liver which were higher than the levels of residues measured in blood. In mice, the highest levels of tissue residues were seen in the adrenal glands. Higher levels of radioactivity, compared to that of whole blood (compared using the *t* test, 20 mg/kg dose group), occurred in mouse adrenal glands and bone marrow and to a lesser extent in mouse kidney, liver, lung, and spleen.

Characterization of Urinary Metabolites. Typical HPLC profiles are shown in Figures 2 and 3. Sulfatase or glucuronidase treatment did not alter the chromatographic profiles of metabolites. Treatment of rat urine with acylase which is reported to have N-deacetylation activity for alkyl mercapturic acids (*33*) and comparison of the HPLC profile before and after treatment showed that most of the components eluting after 25 min in untreated urine were absent and that additional polar peaks were present. The elution times of the components were unaffected in urine which had been incubated in buffer alone. These results indicated that the major eluting components in rat urine were likely to be mercapturic acids, the treatment with acylase removing the *N*-acyl group to produce the more polar cysteine conjugates. HPLC analysis of mouse urine showed that, as for rat, the major components eluting after 25 min (Figure 2) were affected by acylase treatment. In addition to these, mouse urine also contained two significant metabolites eluting around 40 and 50 min (Figure 3). These were not present in rat urine and were resistant to acylase treatment, indicating that they were not mercapturic acids.

Identification of Urinary Metabolites. (1) 2-(*N*-Acetyl-L-cystein-*S*-yl)-1-hydroxybut-3-ene (IIa and IId) and 1-(*N*-Acetyl-L-cystein-*S*-yl)-2-hydroxybut-3-ene (IIb and IIc). HPLC analysis showed four major metabolites in rat and mouse urine eluting between 55 and 80 min (Figures 2 and 3). These disappeared upon

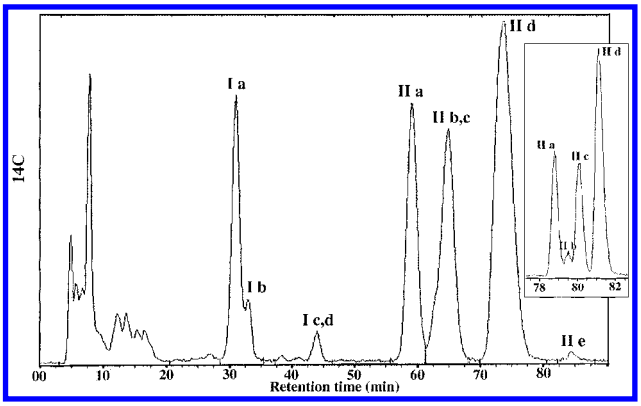

Figure 2. Urinary excretion of [4-^{14}C]BMO metabolites in a male Sprague-Dawley rat, 0−6 h after a single ip administration of 20 mg/kg. For radio-HPLC analysis, we used a YMC ODS AQ column (250 mm × 4.6 mm, 5 μm) and elution was carried out with 1 mM ammonium formate buffer (pH 3) containing acetonitrile (9%) at a flow rate of 1 mL/min. Radioactivity was detected using a flow-through radiodetector (Ramona 90). Individual peaks represent the following: **Ia**, 4-(*N*-acetyl-L-cystein-*S*-yl)-1,2-dihydroxybutane; **Ib**, 4-(*N*-acetyl-L-cystein-*S*-yl)-2-hydroxybutanoic acid; **Ic**, 3-(*N*-acetyl-L-cystein-*S*-yl)propan-1-ol; **Id**, 3-(*N*-acetyl-L-cystein-*S*-yl)propanoic acid; **IIa**, (*R*)-2-(*N*-acetyl-L-cystein-*S*-yl)-1-hydroxybut-3-ene; **IIb**, 1-(*N*-acetyl-L-cystein-*S*-yl)-2-(*S*)-hydroxybut-3-ene; **IIc**, 1-(*N*-acetyl-L-cystein-*S*-yl)-2-(*R*)-hydroxybut-3-ene; **IId**, (*S*)-2-(*N*-acetyl-L-cystein-*S*-yl)-1-hydroxybut-3-ene; and **IIe**, 4-(*N*-acetyl-L-cystein-*S*-yl)-1-hydroxybut-2-ene. The inset shows the further resolution of diastereoisomers **IIa**−**IId**.

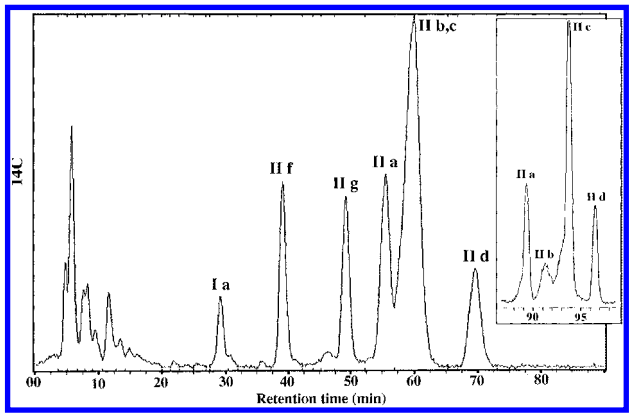

Figure 3. Urinary excretion of [4-^{14}C]BMO metabolites in a male B6C3F1 mouse, 0−6 h after a single ip administration of 20 mg/kg. For radio-HPLC analysis, we used a YMC ODS AQ column (250 mm × 4.6 mm, 5 μm) and elution was carried out with 1 mM ammonium formate buffer (pH 3) containing acetonitrile (9%) at a flow rate of 1 mL/min. Radioactivity was detected using a flow-through radiodetector (Ramona 90). Individual peaks represent the following: **Ia**, 4-(*N*-acetyl-L-cystein-*S*-yl)-1,2-dihydroxybutane; **IIa**, (*R*)-2-(*N*-acetyl-L-cystein-*S*-yl)-1-hydroxybut-3-ene; **IIb**, 1-(*N*-acetyl-L-cystein-*S*-yl)-2-(*S*)-hydroxybut-3-ene; **IIc**, 1-(*N*-acetyl-L-cystein-*S*-yl)-2-(*R*)-hydroxybut-3-ene; **IId**, (*S*)-2-(*N*-acetyl-L-cystein-*S*-yl)-1-hydroxybut-3-ene; **IIf**, *S*-(2-hydroxybut-3-en-1-yl)mercaptoacetic acid; and **IIg**, *S*-(2-hydroxybut-3-en-1-yl)mercaptoacetic acid. The inset shows the further resolution of diastereoisomers **IIa**−**IId**.

incubation with acylase with a concomitant appearance of additional peaks in the polar region of the chromatogram, which categorized them as mercapturic acids. These metabolites were isolated from urine by preparative HPLC and freeze-drying. The GC/MS spectra of their TMS derivatives (Figures 4 and 5) were identical to those of the reference chemicals, 2-(*N*-acetyl-L-cystein-*S*-yl)-1-hydroxybut-3-ene [CI for **IIa** and **IId** *m*/*z* 378 (M + H); EI for **IIa** and **IId** *m*/*z* 362 (M − 15), 318, 308, 287, 234, 228, 103 (CH_2=O^+SiMe_3), 73 (base peak)] and 1-(*N*-

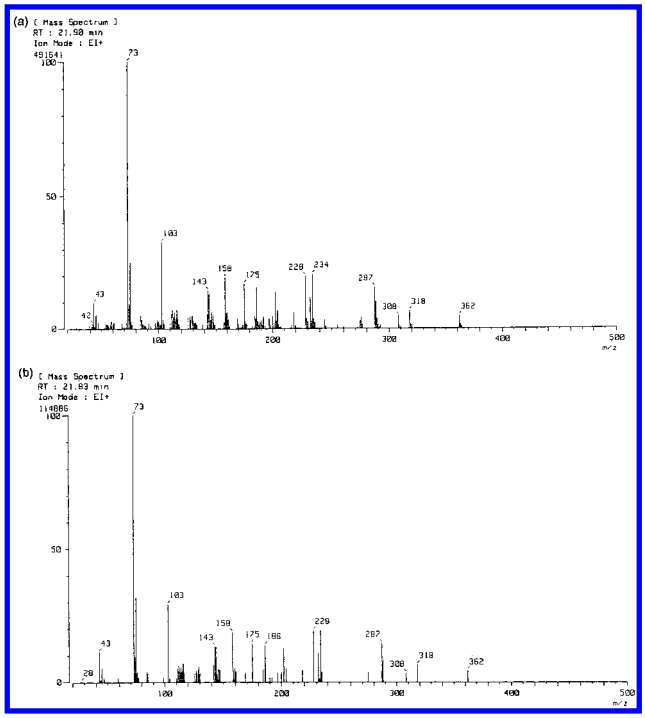

Figure 4. EI mass spectra of the trimethylsilyl derivatives of (a) 2-(*N*-acetyl-L-cystein-*S*-yl)-1-hydroxybut-3-ene diastereoisomers (**IIa** and **IId**) isolated from rat urine and (b) a chemically prepared reference sample.

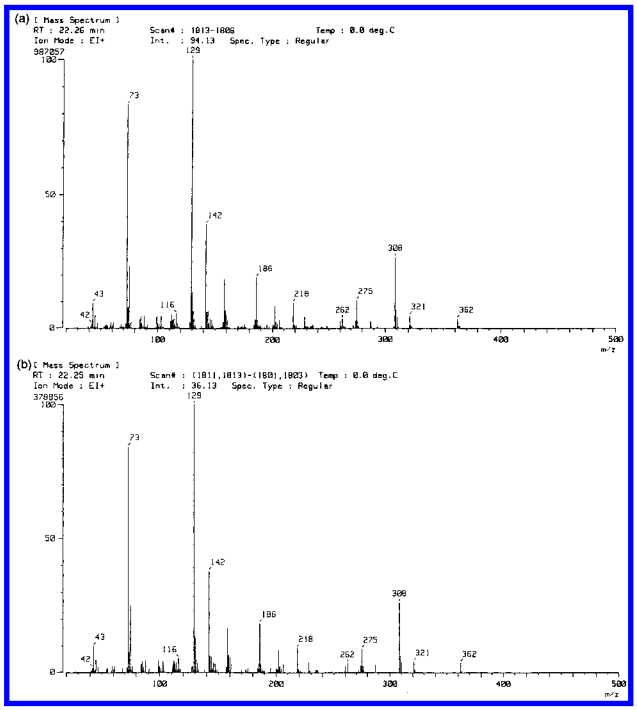

Figure 5. EI mass spectra of the trimethylsilyl derivatives of (a) 1-(*N*-acetyl-L-cystein-*S*-yl)-2-hydroxybut-3-ene diastereoisomers (**IIb** and **IIc**) isolated from rat urine and (b) a chemically prepared reference sample.

acetyl-L-cystein-*S*-yl)-2-hydroxybut-3-ene [CI (methane) for **IIb** and **IIc** *m*/*z* 378 (M + H); EI for **IIb** and **IIc** *m*/*z* 362 (M − 15), 321, 308, 142, 129 (base peak, CH_2=CHCH=O^+SiMe_3)], after derivatization under similar conditions. Radio-LC/MS analysis of rat and mouse urine indicated that the components eluting first and fourth and second and third constituted two pairs of metabolites with the mass spectra showing slightly different fragmentation patterns for each pair. Metabolites 1 and 4 afforded ions at *m*/*z* 234 (M + H), 216, 192, 174, 162, 130, 122, and 105 and metabolites 2 and 3 at *m*/*z* 234 (M + H), 216, 174, 162, and 130. This was the same relative order as seen for a similar analysis of the reference chemicals (see above). Therefore, metabolites 1 and 4 were identified as mercapturic acids arising from the reaction of GSH at C-2 of BMO and metabolites 2 and 3 as mercapturic acids arising from reaction at C-1 (Figures 2 and 3, **IIa** and **IId** and **IIb** and **IIc**, respectively). Cochromatography with reference chemicals using LC/MS identified the first metabolite (**IIa**) in rat and mouse urine as (*R*)-2-(*N*-acetyl-L-cystein-*S*-yl)-1-hydroxybut-3-ene, arising from reaction of GSH at C-2 of (*S*)-BMO, and the second metabolite (**IIb**) as 1-(*N*-acetyl-L-cystein-*S*-yl)-2-(*S*)-hydroxybut-3-ene (**IIb**), arising from reaction at C-1 of (*S*)-BMO. Thus, metabolites **IIc** and **IId** were identified as 1-(*N*-acetyl-L-cystein-*S*-yl)-2-(*R*)-hydroxybut-3-ene (**IIc**) and (*S*)-2-(*N*-acetyl-L-cystein-*S*-yl)-1-hydroxybut-3-ene (**IId**), derived from reaction of GSH at C-1 or C-2 of (*R*)-BMO, respectively.

(2) 4-(*N*-Acetyl-L-cystein-*S*-yl)-1-hydroxybut-2-ene (IIe). A minor metabolite present in rat and mouse urine was tentatively identified as 4-(*N*-acetyl-L-cystein-*S*-yl)-1-hydroxybut-2-ene (**IIe**). This metabolite had chromatographic properties similar to those of a minor component in the reference chemical mixture from the reaction of BMO with NAC, previously identified as **IIe** (*22*). GC/MS of the TMS derivative of this metabolite afforded a spectrum [CI *m*/*z* 378 (M + H); EI *m*/*z* 362 (M − 15), 308, 234, 142, 202, 176,159, 143, 73] corresponding to that of the reference chemical after derivatization under similar conditions which confirmed it was an isomer of (*N*-acetyl-L-cystein-*S*-yl)hydroxybutene.

(3) *S*-(1-Hydroxybut-3-en-2-yl)mercaptoacetic Acid (IIf) and *S*-(2-Hydroxybut-3-en-1-yl)mercaptoacetic Acid (IIg). Two major metabolites present in mouse urine eluting between 40 and 50 min (**IIf** and **IIg**, Figure 3) were not affected by any of the enzyme treatments, indicating that they were not sulfate, glucuronide, or mercapturic acid metabolites of [^{14}C]BMO. Both metabolites were isolated from urine. GC with atomic emission detection (AED, HP5921A) identified the presence of sulfur and the absence of nitrogen in these molecules. The TMS derivatives were analyzed by GC/MS (Figure 6). One metabolite was identified as the TMS derivative of *S*-(1-hydroxybut-3-en-2-yl)mercaptoacetic acid [**IIf**, EI *m*/*z* 306 ($M^{+\bullet}$), 291 (M − 15), 216, 204, 147, 103 (CH_2=O^+SiMe_3), 73 (base peak); CI (methane) *m*/*z* 307 (M + H)], the C-2 isomer. The other metabolite was identified as the TMS derivative of *S*-(2-hydroxybut-3-en-1-yl)mercaptoacetic acid [**IIg**, EI *m*/*z* 306 ($M^{+\bullet}$), 291 (M − 15), 237, 204, 142, 129 (base peak, CH_2=CHCH=O^+-$SiMe_3$), 99, 73; CI (methane) *m*/*z* 307 (M + H)], the C-1 isomer. The structure of these metabolites was confirmed by ^{1}H NMR: ^{1}H NMR of **IIf** (500 MHz, D_2O) 5.72 (1H, ddd, *J* = 17.1, 10, and 9.5 Hz, CH_2=C<u>H</u>CHS), 5.24 (1H, d, *J* = 9.5 Hz, C<u>H$_2$</u>=CH), 5.21 (1H, d, *J* = 17.1 Hz, C<u>H$_2$</u>=CH), 3.71 (2H, m, *J* values could not be obtained, C<u>H$_2$</u>-OH), 3.50 (1H, dt, *J* values could not be obtained, SC<u>H</u>CH$_2$OH), 3.26 (2H, s, SC<u>H$_2$</u>COOH); ^{1}H NMR for **IIg** (500 MHz, D_2O) δ 5.88 (1H, ddd, *J* = 17.1, 10.4, and 6.1 Hz, CH_2=C<u>H</u>CHOH), 5.31 (1H, d, *J* = 17.1 Hz, C<u>H$_2$</u>=CH), 5.21 (1H, d, *J* = 10.4 Hz, C<u>H$_2$</u>=CH), 4.29 (1H, m, SCH$_2$C<u>H</u>OH), 3.24 (2H, s, SC<u>H$_2$</u>COOH), 2.77−2.71 (2H, m, SC<u>H$_2$</u>CHOH).

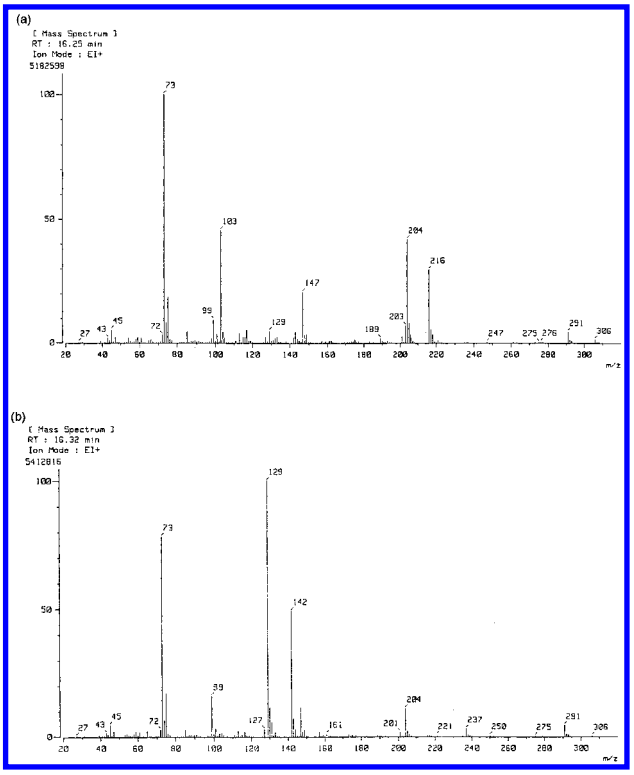

Figure 6. EI mass spectra of the trimethylsilyl derivatives of (a) *S*-(1-hydroxybut-3-en-2-yl)mercaptoacetic acid (**IIf**) and (b) *S*-(2-hydroxybut-3-en-1-yl)mercaptoacetic acid (**IIg**) isolated from mouse urine.

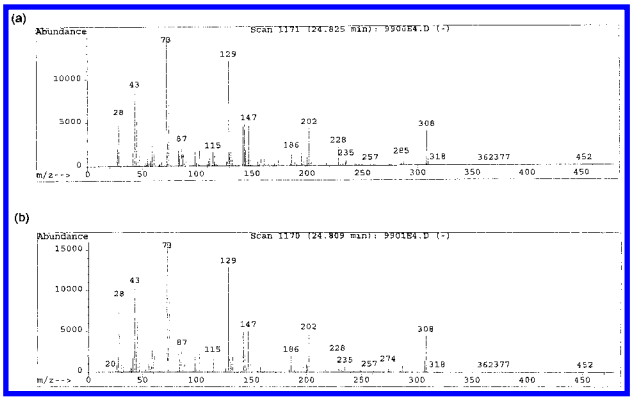

Figure 7. EI mass spectra of the trimethylsilyl derivatives of (a) 4-(*N*-acetyl-L-cystein-*S*-yl)-1,2-dihydroxybutane (**Ia**) isolated from rat urine and (b) a chemically prepared reference sample.

(4) 4-(*N*-Acetyl-L-cystein-*S*-yl)-1,2-dihydroxybutane (Ia) and 4-(*N*-Acetyl-L-cystein-*S*-yl)-2-hydroxybutanoic Acid (Ib). A major metabolite in rat and mouse urine with a retention time between 28 and 35 min (Figures 2 and 3) coeluted with the synthetic standard of 4-(*N*-acetyl-L-cystein-*S*-yl)-1,2-dihydroxybutane, **Ia**. Radio-GC/MS analysis of the TMS derivative of this isolated material afforded a radiolabeled component which gave mass spectra that exactly matched those of the reference chemical (**Ia**) after derivatization under similar conditions (Figure 7). This was therefore identified as the TMS derivative of 4-(*N*-acetyl-L-cystein-*S*-yl)-1,2-dihydroxybutane [EI for **Ia** *m*/*z* 452 (M − 15), 377, 362, 308, 228, 202, 129, 73 (base peak), 43; CI (methane)-for **Ia** *m*/*z* 468 (M + H)]. A second radiolabeled component, present in rat urine only, was identified by radio-GC/MS (Figure 8) as the TMS derivative of 4-(*N*-acetyl-L-cystein-*S*-yl)-2-hydroxybutanoic acid (**Ib**). The mass

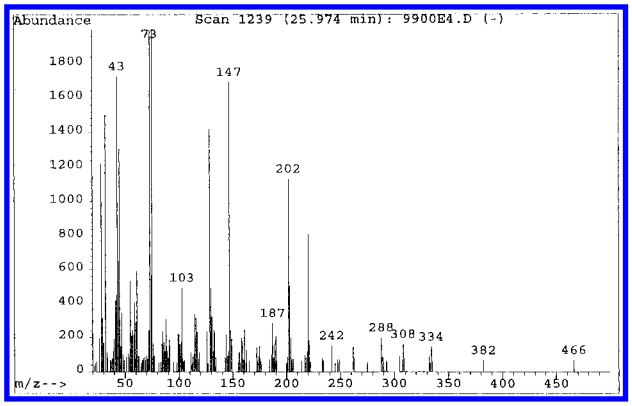

Figure 8. EI mass spectra of the trimethylsilyl derivative of 4-(*N*-acetyl-L-cystein-*S*-yl)-2-hydroxybutanoic acid (**Ib**) isolated from rat urine.

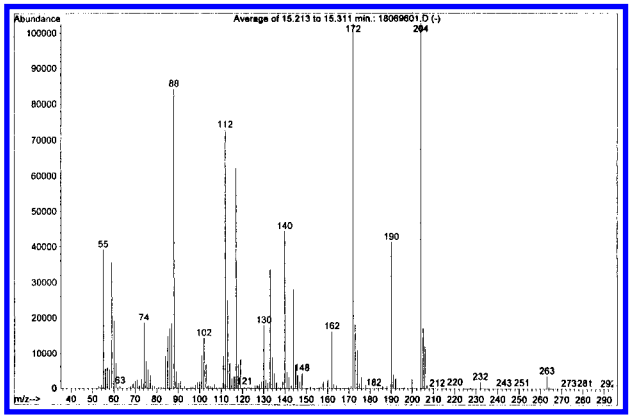

Figure 9. EI mass spectra of 3-(*N*-acetyl-L-cystein-*S*-yl)-propanoic acid (**Id**) isolated from rat urine after methylation.

spectra were consistent with trimethylsilylation of the hydroxyl and carboxyl groups of the metabolite (Figure 8): EI *m*/*z* 466 (M − 15), 334, 308, 220, 202, 147, 129, 103, 73 (base peak), 43; CI (methane) *m*/*z* 482 (M + H). The LC/MS analysis of whole urine confirmed the presence of 4-(*N*-acetyl-L-cystein-*S*-yl)-1,2-dihydroxybutane (**Ia**) in rats and mice [*m*/*z* 250 (M + H)] and 4-(*N*-acetyl-L-cystein-*S*-yl)-2-hydroxybutanoic acid (**Ib**) in rat urine only [*m*/*z* 266 (M + H)].

(5) 3-(*N*-Acetyl-L-cystein-*S*-yl)propan-1-ol (Ic) and 3-(*N*-Acetyl-L-cystein-*S*-yl)propanoic Acid (Id). Two metabolites eluting between 42 and 45 min were present only in rat urine (Figure 2) and were not detected in mouse urine (Figure 3), and these disappeared upon incubation with acylase. Radio-GC/MS analysis of the TMS derivative identified the major radiolabeled component in this fraction isolated from urine as 3-(*N*-acetyl-L-cystein-*S*-yl)propanoic acid [EI for **Id** *m*/*z* 379 ($M^{+\bullet}$), 364 (M − 15), 320, 230, 186, 175, 140, 73 (base peak); CI (methane) for **Id** *m*/*z* 380 (M + H)]. Derivatization of another subsample of the fraction isolated from rat urine by methylation followed by radio-GC/MS analysis (Figure 9) confirmed the presence of a radiolabeled component corresponding to the dimethyl ester of 3-(*N*-acetyl-L-cystein-*S*-yl)propanoic acid [EI for **Id** *m*/*z* 263 ($M^{+\bullet}$), 204, 190, 172, 112, 88 (base peak); CI (methane) for **Id** *m*/*z* 264 (M + H)]. After sequential methylation and acetylation of another sample of this isolated fraction, a second radiolabeled component was detected in addition to the dimethyl ester of **Id**. Mass spectroscopy (Figure 10) identified this as the acylated, methyl ester of 3-(*N*-acetyl-

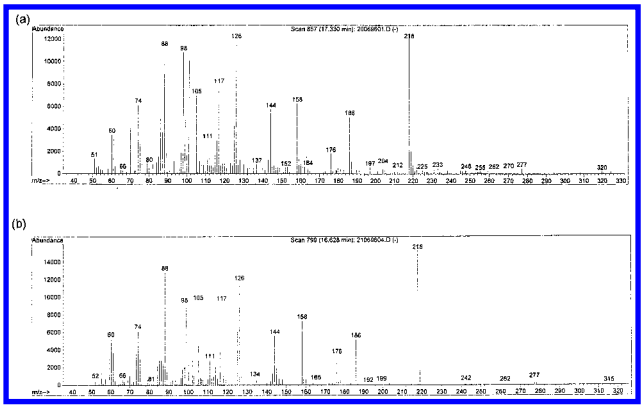

Figure 10. EI mass spectra of (a) 3-(*N*-acetyl-L-cystein-*S*-yl)-propan-1-ol (**Ic**) isolated from rat urine and (b) a chemically prepared reference sample after methylation and acetylation.

L-cystein-*S*-yl)propan-1-ol [EI for **Ic** *m*/*z* 277($M^{+\bullet}$), 218, 186, 158, 126, 88, 43 (base peak); CI (methane) for **Ic** *m*/*z* 278 (M + H)]. The mass spectra were identical to that of the reference chemical, 3-(*N*-acetyl-L-cystein-*S*-yl)propan-1-ol (**Ic**), after derivatization under similar conditions [EI for MS reference chemical *m*/*z* 277 ($M^{+\bullet}$), 218, 186, 158, 126, 88, 43 (base peak); CI (methane) for MS reference chemical *m*/*z* 278 (M + H)]. Selective derivatization, i.e., methylation followed, after MS analysis, by acetylation of the same sample and subsequent MS analysis, such that carboxylic acids afforded methyl esters and alcohols afforded acetoxy derivatives allowed differentiation from other structural assignments consistent with a molecular mass of 263 (**Id**) or 277 (**Ic**). Combinations of additions of 14 in molecular mass (in CI mode) are indicative of the number of carboxyl groups in a molecule; multiples of 42 indicate hydroxyl groups. Thus, the major component was identified as 3-(*N*-acetyl-L-cystein-*S*-yl)propanoic acid (**Id**) and the minor component (ca. 10% of **1d**) as 3-(*N*-acetyl-L-cystein-*S*-yl)propan-1-ol (**Ic**).

Polar Fraction. Radio-LC/MS analysis with selective ion monitoring of the polar fraction of the chromatogram eluting at 0−20 min (Figures 2 and 3) identified two small polar components as the sulfoxides of the isomeric metabolites, 1-(*N*-acetyl-L-cystein-*S*-yl)-2-hydroxybut-3-ene [**IIb** and **IIc**, *m*/*z* 267 (M + NH_4), 250 (M + H), 166, 162, 130] and 2-(*N*-acetyl-L-cystein-*S*-yl)-1-hydroxybut-3-ene [**IIa** and **IId**, *m*/*z* 267 (M + NH_4), 250 (M + H), 166, 162, 130]. These components were also present in samples containing mixtures of metabolites **IIa**−**IId** after periods of intermittent analysis and storage. The sulfoxides were not present when these metabolites were initially isolated. No components corresponding to the reference chemicals 1,2-dihydroxybut-3-ene, 1,3-dihydroxyacetone (Sigma), erythritol (Sigma), 1,3-anhydroerythritol (Sigma), or 4-(*N*-acetyl-L-cystein-*S*-yl)-1,2,3-trihydroxybutane were identified. Comparison of the HPLC profiles before and after acylase treatment of the urine showed that the cysteinyl conjugates produced by deacetylation of the corresponding mercapturic acids eluted slightly after the metabolites in this polar region of the profile. HPLC using a reduced amount of acetonitrile [1 mM ammonium formate buffer (pH 3) containing acetonitrile (3%) at a flow rate of 1 mL/min] of a subsample of the polar region of the urinary metabolic profile after fractionation of the urine showed that it contained a complex mixture of at least 18 minor ^{14}C-labeled metabolites. Under these conditions, the peak eluting at 5−6 min (Figures 2 and 3) was resolved further into several components. Radio-GC/MS after combined methylation and acetylation indicated several peaks containing radioactivity together with a very large quantity of unlabeled components. The total ion chromatogram of this polar fraction was complex, and the resolution of GC radiodetection was insufficient to correlate the radio- and ion chromatograms and assign molecular weights to the radiolabeled components. Little (1−5%) of the radioactivity partitioned from the sample into ethyl acetate under acidic (pH 3), basic (pH 10), or neutral (pH 7) conditions.

Urinary Metabolite Profile. The proportions of individual [^{14}C]BMO metabolites found in the pooled urine samples from the various dose groups are summarized in Table 4. Table 4 serves as an indication of the relative amounts of the metabolites. A more detailed analysis for assessing, for example, the effects of dose would require comparison of individual urine profiles from larger groups of animals which was not the main purpose of this experiment. However, it can be seen that the combined excretion of the regio- and stereoisomers of *N*-acetylcystein-*S*-yl hydroxybutene (**IIa**−**IIe**) accounted for the majority of the radioactivity in both rat and mouse urine (ca. 21−34% of the dose). The major isomer present in rat urine was (*S*)-2-(*N*-acetyl-L-cystein-*S*-yl)-1-hydroxybut-3-ene (**IId**), the C-2 regioisomer derived from (*R*)-BMO. The major isomer present in mouse urine was 1-(*N*-acetyl-L-cystein-*S*-yl)-2-(*R*)-hydroxybut-3-ene (**IIc**), the C-1 isomer derived from (*R*)-BMO. The C-4 isomer, 4-(*N*-acetyl-L-cystein-*S*-yl)-1-hydroxybut-2-ene (**IIe**), accounted for ca. 1% (0.5% of the dose) of the radioactivity in rat urine at all dose levels and was present in smaller amounts in mouse urine. *S*-(1-Hydroxybut-3-en-2-yl)mercaptoacetic acid (**IIf**) and *S*-(2-hydroxybut-3-en-1-yl)mercaptoacetic acid (**IIg**) accounted together for ca. 20% (10% of the dose) of the radioactivity in mouse urine.

Metabolites **Ia**−**Id** accounted together for less than 30% of the urinary radioactivity in both species. The excretion of 4-(*N*-acetyl-L-cystein-*S*-yl)-1,2-dihydroxybutane (**Ia**) and 4-(*N*-acetyl-L-cystein-*S*-yl)-2-hydroxybutanoic acid (**Ib**) accounted for 10−17% (5−8% of the dose) of the radioactivity in rat urine. 4-(*N*-Acetyl-L-cystein-*S*-yl)-1,2-dihydroxybutane (**Ia**) accounted for 6−10% (3−5% of the dose) of the radioactivity in mouse urine. The combined excretion of 3-(*N*-acetyl-L-cystein-*S*-yl)propan-1-ol (**Ic**) and 3-(*N*-acetyl-L-cystein-*S*-yl)propanoic acid (**Id**) in the rat accounted for approximately 3−9% (2−4% of the dose) of the urinary radioactivity (Table 4). 3-(*N*-Acetyl-L-cystein-*S*-yl)propan-1-ol (**Ic**) accounted for ca. 10% of the combined value of **Ic** and **Id**.

Metabolites eluting in the polar fraction of the chromatogram accounted together for ca. 22% (10% of the dose) of the urinary radioactivity in both rats and mice. Individual metabolites in this fraction accounted for less than 1% of the radioactivity.

Discussion

The main objective of this study was to identify the nature of the metabolites of BMO formed by rats and mice so we could use these data to assist in interspecies comparisons and identification of the metabolites of Bd. The study did not seek to simulate blood levels that have occurred in rats and mice following inhalation exposure

Table 4. Urinary Metabolites of [4-^{14}C]BMO after a Single ip Administration of 1, 5, 20, or 50 mg/kg to Male Sprague-Dawley Rats and Male B6C3F1 Mice[a]

		1 mg/kg (0.014 mmol/kg)	5 mg/kg (0.071 mmol/kg)	20 mg/kg (0.286 mmol/kg)	50 mg/kg (0.714 mmol/kg)	mean	regiochemistry
				Rat			
polar[b]		25 (12)[d]	22 (11)	20 (11)	21 (11)	22 ± 2[e]	
pathway I	**Ia** and **Ib**	16 (8)	17 (8)	13 (7)	10 (5)	14 ± 3	
	Ic and **Id**	9 (4)	6 (3)	3 (2)	4 (2)	6 ± 2	
pathway II	**IIa**	12 (6)	12 (6)	14 (7)	14 (7)	13 ± 1	C-2 from (*S*)-BMO
	IIb and **IIc**	13 (6)	16 (8)	21 (11)	25 (13)	19 ± 5	C-1 from (*S*/*R*)-BMO
	IId	22 (11)	26 (13)	28 (15)	24 (12)	25 ± 2	C-2 from (*R*)-BMO
	IIe	1 (0.5)	2 (1)	1 (0.5)	1 (0.5)	1 ± 0.4	
				Mouse			
polar[b]		24 (13)[d]	25 (13)	22 (14)	22 (9)[f]	23 ± 1	
pathway I	**Ia** and **Ib**	10 (5)	6 (3)	6 (4)	6 (3)	10 ± 2	
	Ic and **Id**	–	–	–	–	–	
pathway II	**IIa**	13 (7)	10 (5)	11 (7)	11 (5)	11 ± 1	C-2 from (*S*)-BMO
	IIb and **IIc**	20 (11)	21 (11)	30 (19)	34 (14)	26 ± 6	C-1 from (*S*/*R*)-BMO
	IId	13 (7)	9 (5)	11 (7)	9 (4)	11 ± 2	C-2 from (*R*)-BMO
	IIe	nq[c]	nq	nq	nq		
	IIf	12 (6)	7 (4)	10 (6)	9 (4)	10 ± 2	C-2
	IIg	10 (5)	13 (7)	9 (4)	9 (4)	10 ± 2	C-1

[a] Values are expressed as the mean percentage of the urinary radioactivity recovered ($n = 3$ or 6 rats, $n = 5 \times 5$ mice). [b] For polar, none of the individual metabolites appeared to account for greater than 1% of the recovered urinary radioactivity. [c] nq means not quantified, accounting for less than 0.5% of the urinary radioactivity. [d] Results expressed as a proportion of the administered dose. [e] Mean and SD expressed as a proportion of urinary radioactivity for the four dose groups. [f] Results expressed as a proportion of the administered dose, but the recovery of the urinary radioactivity for this dose group was incomplete.

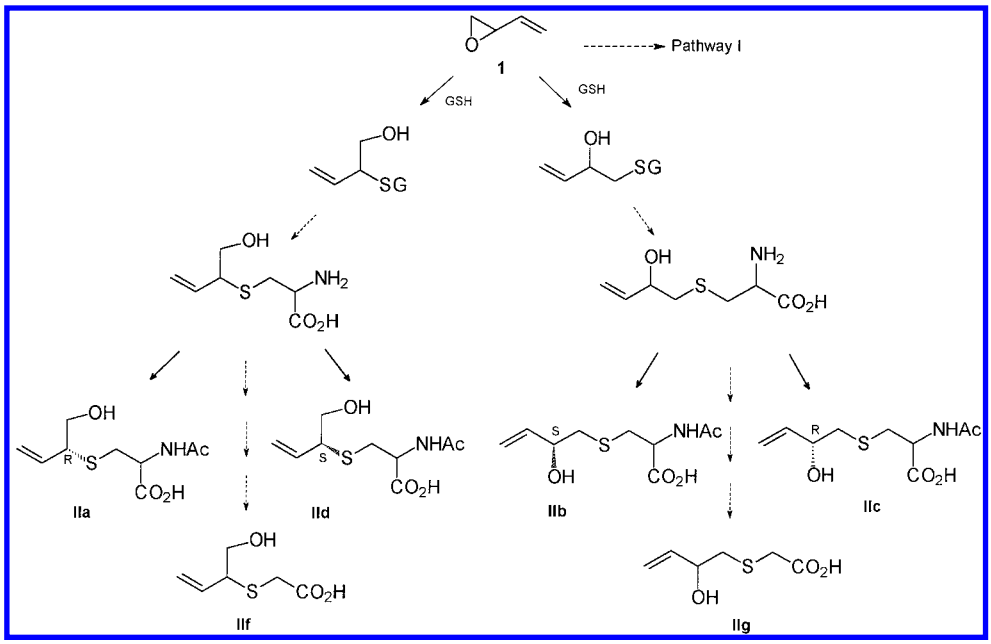

Figure 11. Proposed metabolism of [4-^{14}C]BMO mediated by direct reaction with GSH (pathway II).

to Bd because it is difficult to make direct comparisons between the doses resulting from a single bolus and prolonged inhalation exposure. A range of dose levels were examined to observe the effect of dose on the profile and nature of metabolites. Our results show that rats and mice rapidly metabolize BMO to putatively nongenotoxic intermediates (Figures 11 and 12). The principal initial step of biotransformation in both species was the direct reaction of BMO with GSH (Figure 11, pathway II). Nucleophilic substitution by the thiol at C-1 or C-2 of the epoxide resulted in two diastereomeric pairs of regioisomers, which were excreted as the corresponding mercapturic acids: 1-(*N*-acetyl-L-cystein-*S*-yl)-2-hydroxybut-3-ene (C-1 isomers, **IIb** and **IIc**) and 2-(*N*-acetyl-L-cystein-*S*-yl)-1-hydroxybut-3-ene (C-2 isomers, **IIa** and **IId**). The C-2 isomers (**IIa** and **IId**) predominated in rats, while C-1 isomers (**IIb** and **IIc**) predominated in mice. The differences in the ratios of C-2 and C-1 isomers in rats and mice (Table 5) are probably a result of both chemical and GSH transferase-mediated reactions of GSH with BMO. The C-4 isomer, 4-(*N*-acetyl-L-cystein-*S*-yl)-1-hydroxybut-2-ene (**IIe**), accounted for less than 1% of the administered dose in both rats and mice. It is unclear whether this isomer was formed by the S_N2' reaction of GSH and BMO or by a rearrangement of the C-1 or C-2 metabolites. Although this metabolite had previously been identified from reaction of BMO with NAC, it had not been detected in rat or mouse urine after administration of BMO (*22*). Given the low levels of the C-4 isomer, it is unlikely to have had an effect on the ratios of C-1 and C-2 isomers.

The identification of novel mercaptoacetic acids, *S*-(1-hydroxybut-3-en-2-yl)mercaptoacetic acid (**IIf**) and *S*-(2-hydroxybut-3-en-1-yl)mercaptoacetic acid (**IIg**), in mouse

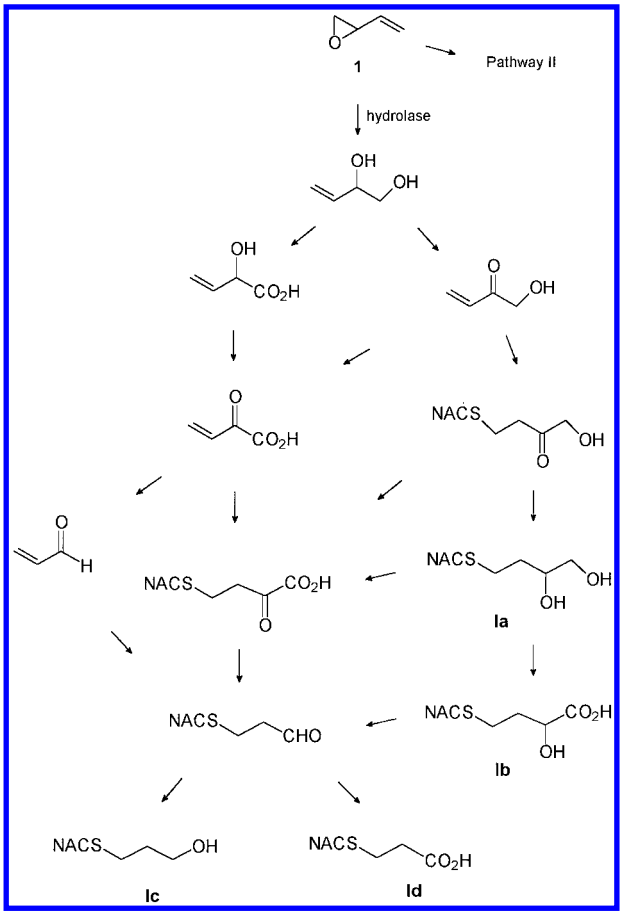

Figure 12. Proposed metabolism of [4-^{14}C]BMO mediated by epoxide hydrolysis (pathway II). Intermediates are not shown, but the pathway may proceed via glutathione, acetyl CoA, or mixed conjugates (NACS is *N*-acetyl-L-cysteine).

urine showed that BMO−cysteine conjugates may, apart from N-acetylation, also undergo deamination (with cysteine conjugate transaminases and L-amino acid oxidases) which yields mercaptopyruvate S-conjugates. Further catabolism of these, by decarboxylases, affords the mercaptoacetic acid metabolites. The mercaptoacetic acid metabolites accounted together for ca. 20% of the urinary radioactivity at all dose levels, and their absence in rat urine is consistent with known species differences in N-acetylation and deamination of cysteine conjugates (*34*, *35*).

A parallel route of metabolism of BMO in both rats and mice is initiated by enzyme hydrolysis and results in the excretion of 4-(*N*-acetyl-L-cystein-*S*-yl)-1,2-dihydroxybutane (**Ia**) in urine (Figure 12, pathway I). This metabolite was identified in the urine of hamsters, mice, rats, and monkeys after inhalation exposure to Bd (*23*, *25*), and it was the only metabolite that could be detected in the urine of people occupationally exposed to Bd (*24*). This study showed that 4-(*N*-acetyl-L-cystein-*S*-yl)-1,2-dihydroxybutane (**Ia**) was also a major metabolite of BMO in rats and mice, in contrast to a previously reported study (*22*) in which this metabolite was not detected after [^{14}C]BMO administration (1−20 mg/kg).

A novel metabolite identified in this study in rat, but not in mouse, urine was 4-(*N*-acetyl-L-cystein-*S*-yl)-2-hydroxybutanoic acid (**Ib**) which can be seen as an oxidation product of 4-(*N*-acetyl-L-cystein-*S*-yl)-1,2-dihydroxybutane (**Ia**, Figure 12) since the xenobiotic portions of GSH conjugates are known to undergo further biotransformation after conjugation (*36*). The formation of **Ia** has been demonstrated to proceed through oxidation of the secondary allylic alcohol of 1,2-dihydroxybutene followed by reaction with GSH (Figure 12) by the use of deuterated substrates (*23*), and the intermediate, 1-hydroxybut-3-en-2-one, has been detected in vitro (*37*). An alternative oxidation product of dihydroxybutene, 2-hydroxybut-3-enoic acid, analogous to mandelic acid formed from the hydrolysis product of styrene oxide (*38*), may also be envisaged. This α-hydroxy acid intermediate could also lead to the formation of 4-(*N*-acetyl-L-cystein-*S*-yl)-2-hydroxybutanoic acid (**Ib**, Figure 12). Two metabolites not previously identified in rat urine were 3-(*N*-acetyl-L-cystein-*S*-yl)propan-1-ol (**Ic**) and 3-(*N*-acetyl-L-cystein-S-yl)propanoic acid (**Id**). Decarboxylation of 4-(*N*-acetyl-L-cystein-*S*-yl)-2-hydroxybutanoic acid (**Ib**) or its precursors would lead to these metabolites via 3-(*N*-acetyl-L-cystein-*S*-yl)propanal (Figure 12). Likewise, decarboxylation of 2-hydroxybut-3-enoic acid followed by conjugation with GSH would also give a route to **Ic** and **Id**.

Recently, Nauhaus et al. (*25*) identified 3-(*N*-acetyl-L-cystein-*S*-yl)propan-1-ol (**Ic**) and 3-(*N*-acetyl-L-cystein-*S*-yl)propanoic acid (**Id**) in mouse but not in rat urine after Bd inhalation exposure (800 ppm, 6 h). The authors suggested that **Ic** and **Id** may be formed from crotonaldehyde via acrolein without the intermediate of BMO and that these aldehydes may contribute to the greater toxicity of Bd in mice. The metabolic formation of crotonaldehyde from Bd has been demonstrated in microsomal incubations (*39*−*42*). Crotonaldehyde and acrolein are cytotoxic, mutagenic, and carcinogenic (*43*−*46*), properties which may attenuate the effects produced by the epoxides of Bd. The presence of 3-(*N*-acetyl-L-cystein-*S*-yl)propan-1-ol (**Ic**) and 3-(*N*-acetyl-L-cystein-S-yl)propanoic acid (**Id**) in this study shows, however, that BMO is the precursor of these metabolites in the rat. Moreover, the corresponding mercapturic acid metabolites of crotonaldehyde, 3-(*N*-acetyl-L-cystein-*S*-yl)-3-methylpropanoic acid and 3-(*N*-acetyl-L-cystein-*S*-yl)-3-methylpropanol (*47*), were not detected in rats or mice. The fact that **Ic** and **Id** were found in the nonsensitive species indicates that intermediates in their formation are nongenotoxic or that the tissue concentrations of these do not reach levels high enough to contribute to the carcinogenicity of Bd. This is in agreement with the proposal that these products were formed through catabolism of conjugated metabolites (Figure 12).

The extent of combined excretion of metabolites derived from hydrolysis (pathway I) was greater in rats than in mice at all dose levels (Table 5) ranging from 14 to 25% (7 to 12% of the dose) of the urinary radioactivity in rats and from 6 to 10% (3 to 5% of the dose) in mice. These results are consistent with the greater epoxide hydrolase activity in rat compared to that in mouse tissue fractions (*8*), although they indicate that both species preferentially metabolized BMO through direct reaction with GSH (pathway II) when it was given by ip injection.

In addition to the activities of the epoxide hydrolase and GSH transferase enzymes which catalyze the initial steps of the biotransformation of BMO, the relative flux through the metabolic pathways may also be governed by the selective formation of stereoisomers. In this study, animals were treated with a racemic mixture of (*R*)- and (*S*)-BMO, but pathway II metabolites originating from the *R*-stereoisomer of BMO (**IIc** and **IId**) predominated over those originating from the *S*-stereoisomer (**IIa** and

Table 5. Ratios of Urinary Metabolites of [4-^{14}C]BMO after a Single ip Administration of 1, 5, 20, or 50 mg/kg to Male Sprague-Dawley Rats and Male B6C3F1 Mice

	ratio of C-2:C-1 isomers[a]	total metabolites pathway I[b] (%)	total metabolites pathway II[c] (%)	ratio of pathway I/total pathway I and II (%)
rat dose level (mg/kg) (mmol/kg)				
1 (0.014)	2.3	25	48	34
5 (0.071)	2.4	23	56	29
20 (0.286)	2.0	16	64	20
50 (0.714)	1.5	14	64	18
		20 ± 5[d]	57 ± 5[d]	
mouse dose level (mg/kg) (mmol/kg)				
1 (0.014)	1.3	10	68	13
5 (0.071)	0.9	6.0	60	9.1
20 (0.286)	0.7	6.0	71	7.8
50 (0.714)	0.6	6.0	72	7.7
		7 ± 2[d]	68 ± 5[d]	

[a] For regioselective formation of metabolites, ratio of C-2:C-1 products (**IIa** and **IId**/**IIb** and **IIc**). [b] For pathway I, the summation of metabolites was derived from epoxide hydrolysis. Values are expressed as the mean percentage of the urinary radioactivity recovered (n = 3 or 6 rats, n = 5 mice). [c] For pathway II, the summation of metabolites was derived from direct reaction with GSH. Values are expressed as the mean percentage of the urinary radioactivity recovered (n = 3 or 6 rats, n = 5 mice). [d] Mean and SD for the four dose groups.

IIb) in both species. This apparent preference for the (*R*)-BMO isomer is consistent with the greater in vitro activity of rat and mouse GSH transferases for (*R*)-BMO and of the competing epoxide hydrolases for (*S*)-BMO (*48*).

Metabolites of DEB or EDB, including those recently reported in rats and mice after Bd inhalation exposure, 3-(*N*-acetyl-L-cystein-*S*-yl)-1,2,4-trihydroxybutane or 1,3-dihydroxyacetone (*25*), or in vitro, 1,3-anhydroerythritol and erythritol (*49*), were not detected by LC/MS in rat or mouse urine in this study. LC/MS showed good sensitivity for the mercapturic acid metabolites. For example, metabolite **IIe** could be detected in mouse urine at levels equivalent to 1% of the urinary radioactivity, and metabolite **Id** could readily be detected in rat urine at levels equivalent to 3% of the urinary radioactivity. The (*N*-acetyl-L-cystein-*S*-yl)trihydroxybutane metabolite measured in mouse urine by Nauhaus (*25*) after exposure to Bd accounted for approximately 5% of the excreted metabolites. The results show that BMO is not an effective intermediate in the formation of DEB or EDB when administered by ip injection and imply that formation of BMO in situ after Bd inhalation exposure must be important in determining further oxidation of the molecule.

Blood levels of radioactivity 48 h after dosing [^{14}C]BMO were higher in rats than in mice. Rats also had higher (up to ca. 10 times) levels of tissue residues than mice at equivalent dose levels, with the highest residues in rat liver. The transient dose-related signs of toxicity observed in rats immediately after receiving doses of BMO at ≥20 mg/kg may stem from secondary effects resulting from enzyme saturation or GSH depletion due to accumulation of BMO. This also raises the possibility that the carcinogenicity of Bd in the rat at very high doses (>1000 ppm, 2 years) is related to the toxicity of its primary metabolite, BMO. The absence of high levels of radioactivity in mouse liver suggests a greater capacity of mice to metabolize BMO to nonreactive metabolites when administered by ip administration.

The identification of novel metabolites and their stereochemistry has revealed quantitative and qualitative differences between male Sprague-Dawley rats and male B6C3F1 mice in the metabolism and disposition of [4-^{14}C]-BMO after ip administration (1−50 mg/kg, 0.014−0.714 mmol/kg).

Factors such as the catabolism of primary metabolites and the selective formation of stereoisomers may govern the flux through metabolic pathways. If, for example, the stereochemistry of BMO as it appears from this work plays a role in steering the metabolic transformations, then simple comparison of enzyme activities may not adequately predict the rates of biotransformation in vivo. Furthermore, it appears that formation of DEB (or EDB) may not be considered two independent reactions of Bd to BMO and BMO to DEB (or EDB), but the overall biotransformation process should be viewed as an integrated step, BD to DEB (or EDB). This provides an explanation for the inability to predict blood BMO and DEB levels after Bd exposure when these are calculated using PBPK models based on metabolic rates for the individual reactions (*26*). These factors should be taken into account when interpreting mathematical models developed for quantitative risk assessment and extrapolation of animal data to humans.

Acknowledgment. We acknowledge the valuable assistance of M. E. Cheeseman (Shell Research Centre, Sittingbourne), A. M. P. Ross, G. J. van Velzen, and W. J. L. Genuit (Analytical Department, Shell Research and Technology Centre, Amsterdam), and C. Bleasdale, K. F. Handley and R. G. Young (Department of Chemistry, University of Newcastle upon Tyne).

References

(1) Owen, P. E. (1981) The toxicity and carcinogenicity of butadiene gas administered to rats by inhalation for approximately 24 months. Hazelton Laboratories Europe Technical Report 2653-522/2, International Institute of Synthetic Rubber Producers, Houston, TX.

(2) U.S. National Toxicology Program (1984) Toxicology and carcinogenesis studies of 1,3-butadiene (CAS registry number 106-99-0) in B6C3F1 mice (inhalation studies). TR 288 NIH 84-2544, U.S. National Toxicology Program, Research Triangle Park, NC.

(3) Owen, P. E., Glaister, J. R., Gaunt, I. F., and Pullinger, D. H. (1987) Inhalation toxicity studies with 1,3-butadiene. III. Two year toxicity/carcinogenicity study in rats. *J. Am. Ind. Hyg. Assoc.* **48**, 407−413.

(4) Owen, P. E., and Glaister, J. R. (1990) Inhalation toxicity and carcinogenicity of 1,3-butadiene in Sprague-Dawley rats. *Environ. Health Perspect.* **86**, 19−25.

(5) U.S. National Toxicology Program (1993) Toxicology and carcinogenesis studies of 1,3-butadiene (CAS registry number 106-99-0) in B6C3F1 mice (inhalation studies). TR 434 NIH 93-3165, National Toxicology Program, Research Triangle Park, NC.

(6) Malvoisin, E., Lhoest, G., Poncelet, F., Roberfroid, M., and Mercier, M. (1979) Identification and quantitation of 1,2-epoxybutene-3 as the primary metabolite of 1,3-butadiene. *J. Chromatogr.* **178**, 419−425.

(7) Malvoisin, E., and Roberfroid, M. (1982) Hepatic microsomal metabolism of 1,3-butadiene. *Xenobiotica* **12**, 137−144.
(8) Csanády, G. A., Guengerich, F. P., and Bond, J. A. (1992) Comparison of the biotransformation of 1,3-butadiene and its metabolite, butadiene monoepoxide, by hepatic and pulmonary tissues from humans, rats and mice. *Carcinogenesis* **13**, 1143−1153.
(9) Schmidt, U., and Loeser, E. (1982) Species differences in the formation of butadiene monoxide from 1,3-butadiene. *Arch. Toxicol*. **57**, 222−225.
(10) Bolt, H. M., Schmiedel, G., Filser, J. G., Rolzhäuser, H. P., Lieser, K., Wistuba, D., and Schurig, V. (1983) Biological activation of 1,3-butadiene to vinyl oxirane by rat liver microsomes and expiration of the reactive metabolite by exposed rats. *Cancer Res. Clin. Oncol*. **106**, 112−118.
(11) Himmelstein, M. W., Asgharian, B., and Bond, J. A. (1995) High concentrations of butadiene epoxides in livers and lungs of mice compared to rats exposed to 1,3-butadiene. *Toxicol. Appl. Pharmacol*. **132**, 281−288.
(12) Thornton-Manning, J. R., Dahl, A. R., Bechtold, W. E., Griffith, W. C., Jr., and Henderson, R. F. (1995) Disposition of butadiene monoepoxide and butadiene diepoxide in various tissues of rats and mice following a low-level inhalation exposure to 1,3-butadiene. *Carcinogenesis* **16**, 1723−1731.
(13) Dahl, A. R., Bechtold, W. E., Bond, J. A., Henderson, R. F., Mauderly, J. L., Muggenburg, B. A., Sun, J. D., and Birnbaum, L. S. (1990) Species differences in the metabolism and disposition of inhaled 1,3-butadiene and isoprene. *Environ. Health Perspect*. **86**, 65−69.
(14) Thornton-Manning, J. R., Dahl, A. R., Bechtold, W. E., Griffith, W. C., Jr., Pei, L., and Henderson, R. F. (1995) Gender differences in the metabolism of 1,3-butadiene in Sprague-Dawley rats following a low-level inhalation exposure. *Carcinogenesis* **16**, 2875−2878.
(15) Thornton-Manning, J. R., Dahl, A. R., Bechtold, W. E., and Henderson, R. F. (1996) Gender and species differences in the metabolism of 1,3-butadiene to butadiene monoepoxide and butadiene diepoxide in rodents following a low-level inhalation exposure. *Toxicology* **112**, 1−4.
(16) Himmelstein, M. W., Turner, M. J., Asgharian, B., and Bond, J. A. (1994) Comparison of blood concentrations of 1,3-butadiene and butadiene epoxides in mice and rats exposed to 1,3-butadiene. *Carcinogenesis* **15**, 1479−1486.
(17) Bechtold, W. E., Strunk, M. R., Thornton-Manning, J. R., and Henderson, R. F. (1995) Analysis of butadiene, butadiene monoepoxide butadiene diepoxide in blood by gas chromatography/gas chromatography/mass spectroscopy. *Chem. Res. Toxicol*. **8**, 182−187.
(18) Cochrane, J. E., and Skopek, T. R. (1994) Mutagenicity of 1,3-butadiene and its epoxide metabolites. I. Mutagenic potential of 1,2-epoxybutene, 1,2,3,4-diepoxide and 3,4-epoxy-1,2-butanediol in cultured human lymphoblasts. *Carcinogenesis* **15**, 713−717.
(19) Millard, J. T., and White, M. M. (1993) Diepoxybutane cross-links DNA at 5-GNC sequences. *Biochemistry* **32**, 2120−2124.
(20) ECETOC (1993) No 4,1,3-Butadiene Criteria Document, Brussels, Belgium.
(21) Himmelstein, M. W., Acquavella, J. F., Recio, L., Medinsky, M. A., and Bond, J. A. (1997) Toxicology and epidemiology of 1,3-butadiene. *Crit. Rev. Toxicol*. **27**, 1−108.
(22) Elfarra, A. A., Sharer, J. E., and Duescher, R. J. (1995) Synthesis and characterisation of *N*-acetyl-L-cysteine-S-conjugates of butadiene monoxide and their detection and quantitation in urine of rats and mice given butadiene monoxide. *Chem. Res. Toxicol*. **8**, 68−76.
(23) Sabourin, P. J., Burka, L. T., Bechtold, W. E., Dahl, A. R., Hoover, M. D., Chang, I.-Y., and Henderson, R. F. (1992) Species differences in urinary butadiene metabolites: Identification of 1,2-dihyroxy-4-(*N*-acetylcysteinyl)butane. *Carcinogenesis* **13**, 1633−1638.
(24) Bechtold, W. E., Strunk, M. R., Chang, I.-Y., Ward, J. B., Jr., and Henderson, R. F. (1994) Species differences in urinary butadiene metabolites: comparison of metabolite ratios between mice, rats and humans. *Toxicol. Appl. Pharmacol*. **127**, 44−49.
(25) Nauhaus, S. K., Fennell, T. R., Asgharin, B., Bond, J. A., and Sumner, S. C.-J. (1996) Characterisation of urinary metabolites from Sprague-Dawley rats and B6C3F1 mice exposed to [1,2,3,4-^{13}C]butadiene. *Chem. Res. Toxicol*. **9**, 764−773.
(26) Sweeney, L. M., Schlosser, P. M., Medinsky, M. A., and Bond, J. A. (1997) Physiologically based pharmacokinetic modeling of 1,3-butadiene, 1,2-epoxy-3-butene and 1,2:3,4-diepoxybutane toxicokinetics in mice and rats. *Carcinogenesis* **18**, 611−625.
(27) De Meester, C., Poncelet, F., Roberfroid, M., and Mercier, M. (1978) Mutagenicity of butadiene and butadiene monoxide. *Biochem. Biophys. Res. Commun*. **80**, 298−305.
(28) Sharief, Y., Brown, A. M., Backer, L. C., Campbell, J. A., Westbrook-Collins, B., Stead, A. G., and Allen, J. W. (1986) Sister-chromatic exchange and chromosome aberration analysis in mice after *in vivo* exposure to acetonitrile, styrene or butadiene monoxide. *Environ. Mutagen*. **4**, 439−448.
(29) Ramu, K., Fraiser, L. H., Mamiya, B., Ahmed, T., and Kehrer, J. P. (1995) Acrolein mercapturates: Synthesis, characterization and assessment of their role in the bladder toxicity of cyclophosphamide. *Chem. Res. Toxicol*. **8**, 515−524.
(30) Golding, B. T., Slaich, P. K., Kennedy, G., Bleasdale, C., and Watson, W. P. (1996) Mechanisms of formation of adducts from reactions of glycidaldehyde with 2′-deoxyguanosine and/or guanosine. *Chem. Res. Toxicol*. **9**, 147−157.
(31) Hennion, G. F., and Kupiecki, F. P. (1953) Some reactions of 2-butane-1,4-diol. *J. Org. Chem*. **18**, 1601−1609.
(32) Neagu, C., and Hase, T. (1993) Synthesis of enantiomerically pure 3-butene-1,2-diol derivatives via a Sharpless asymmetric epoxidation route. *Tetrahedron Lett*. **34** (10), 1629−1630.
(33) Tateishi, M. (1983) Acylase I and III. *Drug Metab. Rev*. **14**, 1207−1211.
(34) Harris, G. L. A., James, S. P., and Needham, D. (1968) The formation of 3-(butyl-thio)-lactate. *Biochem. J*. **108**, 7P.
(35) Reichert, D., Schutz, S., and Metzler, M. (1985) Cystein conjugate toxicity, metabolism, and binding to macromolecules in isolated rat kidney mitochondria. *Biochem. Pharmacol*. **34**, 499−505.
(36) Mitchell, D. Y., and Peterson, D. R. (1989) Metabolism of the glutathione-acrolein adduct, S-(2-aldehydo-ethyl)glutathione, by rat liver alcohol and aldehyde dehydrogenase. *J. Pharmacol. Exp. Ther*. **251**, 193−198.
(37) Kemper, R. A., Krause, R. J., and Elfarra, A. A. (1997) Oxidation of 3-butene-1,2-diol by mouse, rat and human liver microsomes. *Fundam. Appl. Toxicol*. **36** (Suppl. Toxicologist), 317.
(38) Sumner, S. C. J., and Fennell, T. R. (1994) Review of the metabolic fate of styrene. *Crit. Rev. Toxicol*. **24** (S1), S11−S33.
(39) Elfarra, A. A., Sharer, J. E., and Duescher, R. J. (1991) Mechanisms of 1,3-butadiene oxidations to butadiene monoxide and crotonaldehyde by mouse liver microsomes and chloroperoxidase. *Arch. Biochem. Biophys*. **286**, 244−251.
(40) Sharer, J. E., Duescher, R. J., and Elfarra, A. A. (1992) Species and tissue differences in the microsomal oxidation of 1,3-butadiene and the glutathione conjugation of butadiene monoepoxide in mice and rats: possible role in 1,3-butadiene-induced toxicity. *Drug Metab. Dispos*. **20**, 658−664.
(41) Cheng, X., and Ruth, R. A. (1993) A simplified methodology for the quantitation of butadiene metabolites: application to the study of 1,3-butadiene metabolism by rat liver microsomes. *Drug Metab. Dispos*. **21**, 121−124.
(42) Duescher, R. J., and Elfarra, A. A. (1994) Human liver microsomes are efficient catalysts for 1,3-butadiene oxidation: evidence for major roles by cytochrome P450 2A6 and 2E1. *Arch. Biochem. Biophys*. **311**, 342−349.
(43) Witz, G. (1989) Biological interactions of α,β-unsaturated aldehydes. *Free Radical Biol. Med*. **7**, 333−349.
(44) Eder, E., Henschler, D., and Neudecker, T. (1982) Mutagenic properties of allylic and α,β-unsaturated compounds: consideration of alkylating mechanisms. *Xenobiotica* **12**, 831−848.
(45) Chung, F.-L., Young, R., and Hecht, S. S. (1984) Formation of cyclic 1,N^2-propanodeoxyguanosine adducts in DNA upon reaction with acrolein and crotonaldehyde. *Cancer Res*. **44**, 990−995.
(46) Marnett, L. J., Hurd, H. K., Hollstein, M. C., Levin, D. E., Esterbauer, H., and Ames, B. N. (1985) Naturally occurring carbonyl compounds are mutagens in *Salmonella* tester strain TA 104. *Mutat. Res*. **148**, 25−34.
(47) Gray, J. M., and Barnsley, E. A. (1971) The metabolism of crotyl phosphate, crotyl alcohol and crotonaldehyde. *Xenobiotica* **1**, 55−67.
(48) Wistuba, D., and Schurig, V. (1986) Complementary epoxide hydrolase vs glutathione S-transferase-catalyzed kinetic resolution of simple aliphatic oxiranes: complete regio- and enantioselective hydrolysis of *cis*-2-ethyl-3-methyloxirane. *Angew. Chem., Int. Ed*. **25**, 1032−1034.
(49) Boogaard, P. J., and Bond, J. A. (1996) The role of hydrolysis in the detoxification of 1,2:3,4-diepoxybutane by human, rat and mouse liver and lung *in-vitro*. *Toxicol. Appl. Pharmacol*. **141**, 617−627.

TX970175V